Acta Crystallographica Section A
Foundations of Crystallography
ISSN 0108-7673

Received 6 June 2011
Accepted 10 August 2011

The paper is dedicated to Heinz Jagodzinski on the occasion of his 95th birthday.

The application of *eigensymmetries* of face forms to X-ray diffraction intensities of crystals twinned by 'reticular merohedry'

H. Klapper* and Th. Hahn

Institut für Kristallographie, RWTH Aachen University, D-52056 Aachen, Germany. Correspondence e-mail: klapper@xtal.rwth-aachen.de

This paper is an extension of a previous treatment of 'twins by merohedry' with full lattice coincidence [$\Sigma = 1$, Klapper & Hahn (2010). *Acta Cryst.* A**66**, 327–346] to 'twins by reticular merohedry' with partial lattice coincidence ($\Sigma > 1$). Again, the sets of symmetrically equivalent reflections $\{hkl\}$ are considered as sets of equivalent faces (face forms) $\{hkl\}$, and the behaviour of the *oriented eigensymmetries* of these forms under the action of a twin operation is used to determine the X-ray reflection sets, the intensities of which are affected or not affected by the twinning. The following cases are treated: rhombohedral obverse/reverse $\Sigma 3$ twins, cubic $\Sigma 3$ (spinel) twins, tetragonal $\Sigma 5$ twins (twin elements $m'(120)$, $2'[\bar{2}10]$) and hexagonal $\Sigma 7$ twins ($m'(12\bar{3}0)$, $2'[2\bar{1}0]$). For each case the twin laws for all relevant point groups are defined, and the twin diffraction cases A (intensity of twin-related reflection sets not affected), B1 (intensity affected), B2 (intensity affected only by anomalous scattering) and S (single, *i.e. non-coincident* reflection sets) are derived for all twin laws. A special treatment is provided for the cubic $\Sigma 3$ twins, where the cubic face forms first have to be split into up to four rhombohedral subforms with a threefold axis along one of the four cube $\langle 111 \rangle$ directions, here [111]. These subforms exhibit different twin diffraction cases analogous to those derived for the rhombohedral obverse/reverse $\Sigma 3$ twins. A complete list of the split forms and their diffraction cases for all cubic point groups and all $\Sigma 3$ twin elements is given. The application to crystal structure determination of crystals twinned by reticular merohedry and to X-ray topographic mapping of twin domains is discussed.

1. Introduction

In this contribution we deal with '*twinning by reticular* (*or lattice*) *merohedry*' (Friedel, 1926, p. 444; Hahn & Klapper, 2003, Sections 3.3.8 and 3.3.9), which is the extension of a previous article on the *twinning by* (*strict*) *merohedry* ($\Sigma = 1$) (Klapper & Hahn, 2010) to the case of 'twinning with partial lattice coincidence' (lattice index $\Sigma > 1$). In order to avoid repetitions, the reader is asked to read the former paper. Here we briefly repeat only the fundamental ideas and results of that contribution.

(i) A face form (crystal form) $\{hkl\}$ is the set of all crystal faces that are symmetrically equivalent with respect to the point group $\mathcal{G}$ of the crystal. The *eigensymmetry* $\mathcal{H}$ ('shape symmetry') of a face form is the point group of the face form. It is a proper or improper supergroup of the generating point group: $\mathcal{G} \leq \mathcal{H}$. Example: the tetragonal prism $\{100\}$ generated by point group $\mathcal{G} = 4$ has the *eigensymmetry* $\mathcal{H} = 4/m2/m2/m$. The other tetragonal prisms $\{110\}$ and $\{hk0\}$ exhibit the same type of *eigensymmetry,* but have different '*oriented eigensymmetries*'. Of particular significance are the non-centrosymmetric face forms.[1]

(ii) We illustrate an X-ray reflection hkl by the corresponding crystal face (hkl) and a set $\{hkl\}$ of symmetrically equivalent reflections by the corresponding face form $\{hkl\}$. Since all reflections of the set corresponding to a face form are symmetrically equivalent, they have the same structure-factor moduli $|F|$. Reflection sets $\{hkl\}$ of *non-centrosymmetric* face forms are *acentric, i.e.* 'opposite' reflections hkl and $\overline{hkl}$ are not symmetrically equivalent and have therefore different F moduli, owing to different (possibly small) anomalous scattering contributions (*Bijvoet pairs*). Reflections belonging to *centrosymmetric* face forms are *centric*, *i.e.* opposite reflections

[1] A complete listing of all general and special face forms of the 32 point groups is given in ch. 10 of Hahn & Klapper (2002), Table 10.1.2.2; the *eigensymmetries* of the 47 face forms are listed in Table 10.1.2.3. Illustrations of all face forms are contained in ch. 3.2 (pp. 184–188) of the book by Vainshtein (1994), ch. 3 (Fig. 73) of Shubnikov & Koptsik (1974) and ch. 10 of Buerger (1956).

hkl and $\overline{hkl}$ belong to the same face form: they are equivalent and have the same F moduli (*Friedel pairs*).

(iii) The correspondence of reflection sets and face forms is applied to illustrate the intensity relations of X-ray reflections of crystals twinned by (strict) merohedry ($\Sigma = 1$). Here, the twin operation is a symmetry operation of the lattice point group (holohedry), *i.e.* the lattices of the two twin components are completely mapped upon themselves, and so are their reciprocal lattices. Thus, all different twin domains are simultaneously in an exact reflection position for all reflections hkl, and their intensities are superimposed. Two kinds, A and B, of reflections hkl are distinguished in terms of the *eigensymmetry* of their corresponding face form $\{hkl\}$:

'*Twin diffraction case A*': the twin element is a symmetry element of the oriented *eigensymmetry* of the face form $\{hkl\}$, *i.e.* the face form is mapped upon itself by the twinning, and so is the set of corresponding reflections, *i.e.* the twin-related superimposed reflections are *symmetrically equivalent* and have the same structure-factor moduli $|F|$. The intensity of this kind of superimposed reflection is independent of the volume ratio of the twin components, and in X-ray topography there is no 'area contrast' of the twin domains.

'*Twin diffraction case B*': the twin element is *not* a symmetry element of the oriented *eigensymmetry* of the face form, *i.e.* the form is not mapped upon itself and the corresponding twin-related reflections are *not symmetrically equivalent* and, hence, have different F moduli. The intensity of these superimposed reflections depends on the volume ratio of the twin components, and in X-ray topography the twin domains are distinguished by 'area contrast'.

Diffraction case B is further subdivided into cases B1 and B2:

Diffraction case B1: the face form $\{hkl\}$ is *not* mapped by the twin operation upon itself *nor*, if non-centrosymmetric, upon its inverse ('*opposite*') form $\{\overline{hkl}\}$ (see case B2 below). Thus, the *geometric structure factors are different* and so are the superimposed intensities of these twin-related reflections.

Diffraction case B2: the face form $\{hkl\}$ is non-centrosymmetric and mapped by the twin operation upon its 'opposite' form $\{\overline{hkl}\}$: the F moduli of the twin-related reflections differ *only due to their different anomalous-scattering contributions*, whereas the geometric parts of the structure factors are equal (*Bijvoet sets*). In the case of low anomalous scattering the difference between the two F moduli may be negligible.

In the previous paper (Klapper & Hahn, 2010), these cases and their applications are fully treated, with examples and a complete listing of all 63 cases of twins by (strict) merohedry ($\Sigma = 1$). These results are now supplemented by the following statement concerning the effect of systematic space-group extinctions on the intensities of superimposed twin-related reflections:

If there are reflection conditions ('systematic extinctions') due to cell centring, glide planes or screw axes, a (twinning) coincidence of non-extinct ('present') reflections of one domain with extinct ('absent') twin-related reflections of the other domain, and *vice versa*, does *not occur*. The $\Sigma1$ twin operations map non-extinct on non-extinct and extinct on extinct reflections, with *one single exception* among all space groups: the cubic space group $P2_1/a\overline{3}$ with $\Sigma1$ twin law $2/m\overline{3} \rightarrow 4/m\overline{3}2/m$. Because of the a glide, twin-related reflection sets $\{0kl\}$ and $\{k0l\}$[2] (non-equivalent pentagon-dodecahedra) obey the reflection conditions $k = 2n$ and $l = 2m$, respectively. Thus, for sets $\{0kl\}$ and $\{k0l\}$ with *mixed* even and odd k and l, one of the superimposed sets is always extinct, whereas pairs with both k, l odd are extinct and with both k, l even are 'present'. This holds for all reflections of the set (*i.e.* for all cyclic permutations of 0, k, l).

It is finally emphasized that face forms and their *eigensymmetries* are used here to *illustrate* geometrically the sets of equivalent reflections (all having the same F moduli) and their symmetries.[3] They do *not provide any information* about the absolute values of the reflection intensities. A face form $\{hkl\}$ represents all orders nh, nk, nl of a reflection hkl, independent of their F moduli, including those reflection orders which are extinct (*i.e.* $|F| = 0$). In the following we use the symbol $\{hkl\}$ synonymously for face forms *and* reflection sets.

2. Twins by reticular merohedry

2.1. Basic features, examples

In twinning by *reticular merohedry* the twin operation is *not* a symmetry operation of the lattice symmetry (holohedry), but maps only a part of the two twin-related lattices upon each other, thus forming a common *sublattice* ('*coincidence-site lattice*' or '*twin lattice*') of lattice index $[j] = \Sigma m = V_{\rm twin}/V_{\rm crystal} > 1$ (j or m is the volume ratio of the primitive unit cells of the twin lattice and of the original 'untwinned' crystal lattice, Hahn & Klapper, 2003, p. 417). Since the translation group of this sublattice is a subgroup of the single-domain lattice, Friedel (1926) has coined the term '*twinning by reticular* (*lattice*) *merohedry*' ('*macles par mériédrie réticulaire*').

Regarding the coincidence and overlap of twin-related X-ray reflections, there is an essential difference between twins by (strict) merohedry ($\Sigma = 1$) and twins by reticular merohedry ($\Sigma > 1$). For $\Sigma1$ twins, because of the *complete* coincidence of the two crystal lattices, *all* reciprocal-lattice points of one crystal coincide with reciprocal-lattice points of its twin-related counterpart. In contrast, for twins by reticular merohedry ($\Sigma > 1$) the reciprocal lattices of the twin partners overlap only partially. Their diffraction patterns can be described in two ways:

(*a*) In terms of the unit cells of the two twin partners [domain states D(I) and D(II)] with basis vectors $\mathbf{a}_1$, $\mathbf{b}_1$, $\mathbf{c}_1$ and $\mathbf{a}_2$, $\mathbf{b}_2$, $\mathbf{c}_2$ and transformation $(\mathbf{a}_2, \mathbf{b}_2, \mathbf{c}_2) = (\mathbf{a}_1, \mathbf{b}_1, \mathbf{c}_1) \times \mathcal{T}$ (matrix notation, $\mathcal{T} = 3 \times 3$ transformation matrix of the twin operation). The twin-related reflection indices $h_1k_1l_1$ and $h_2k_2l_2$ are transformed accordingly: $(h_2k_2l_2) = (h_1k_1l_1) \times \mathcal{T}$. Since $\mathcal{T}$ is *not* a symmetry operation of the lattice, it leads to integer *as well as* to fractional indices $h_2k_2l_2$. Three integer

[2] Representative twin operation $m'(1\overline{1}0)$.

[3] Note that this illustration does not require crystals to exhibit planar (habit) faces and complete face forms. It is applicable to crystals of any (also spherical) shape to be studied by X-ray diffraction. This is shown in Section 2.3, p. 336, of Klapper & Hahn (2010).

indices represent 'coincident' (overlapping) reflections $h_1k_1l_1$ and $h_2k_2l_2$ of D(I) and D(II), whereas the occurrence of at least one fractional index[4] of h_2, k_2 or l_2 indicates that this reflection is 'absent', *i.e.* there is no reflection $h_2k_2l_2$ coinciding with reflection $h_1k_1l_1$ of domain D(I). The latter are called 'single' reflections. Similarly, by the inverse transformation $(h_1k_1l_1) = (h_2k_2l_2) \times \mathcal{T}^{-1}$ the same set of *coincident* reflections $h_1k_1l_1/h_2k_2l_2$ as before is obtained. The single reflections, however, are now $h_2k_2l_2$ of domain D(II).

(*b*) In terms of the Σm cell of the coincidence lattice with basis vectors $\mathbf{a}_m$, $\mathbf{b}_m$, $\mathbf{c}_m$. The basis transformations from the two twin-related unit cells of D(I) and D(II) are given by: $(\mathbf{a}_m, \mathbf{b}_m, \mathbf{c}_m) = (\mathbf{a}_1, \mathbf{b}_1, \mathbf{c}_1) \times \mathcal{M}_1$ and $(\mathbf{a}_m, \mathbf{b}_m, \mathbf{c}_m) = (\mathbf{a}_2, \mathbf{b}_2, \mathbf{c}_2) \times \mathcal{M}_2$ [$\mathcal{M}_1$ and $\mathcal{M}_2$ are 3×3 matrices with determinant m]. The corresponding transformations of reflection indices are $(HKL) = (h_1k_1l_1) \times \mathcal{M}_1$ and $(HKL) = (h_2k_2l_2) \times \mathcal{M}_2$. Reference to this coincidence-lattice coordinate system has the great practical advantage that all coincident and single reflections of both domain states D(I) and D(II) appear with integer indices HKL. There are, however, 'extinctions' of reflections of both domain states D(I) and D(II). These can be derived from the above *inverse* index transformations $(h_1k_1l_1) = (HKL) \times \mathcal{M}_1^{-1}$ for D(I) and $(h_2k_2l_2) = (HKL) \times \mathcal{M}_2^{-1}$ for D(II). These transformations lead to both integer and fractional indices $h_1k_1l_1$ and $h_2k_2l_2$. Those HKL leading to integer hkl are 'non-extinct' (present), whereas those HKL leading to fractional hkl are 'extinct'. Note that these reflection conditions ('non-extinction conditions', in the following abbreviated as NOC) are different for D(I) and D(II).

Applying the NOC of (*b*) above to Σm reticular twins, four different types of reflections HKL, based on the coincidence-lattice cell $\mathbf{a}_m$, $\mathbf{b}_m$, $\mathbf{c}_m$, can be distinguished with respect to their coincidence and extinction behaviour:

(i) the reflection HKL fulfils simultaneously the NOC of D(I) and D(II): *both* twin-related D(I) and D(II) reflections are non-extinct, *i. e.* coincident (superimposed);

(ii) the reflection HKL fulfils the NOC only for D(I): the reflection is extinct (absent) in D(II), *i.e.* HKL is a 'single' D(I) reflection;

(iii) the reflection HKL fulfils the NOC only of D(II): the reflection is extinct (absent) in D(I), *i.e.* HKL is a 'single' D(II) reflection;

(iv) the reflection HKL does not fulfil the NOC of either D(I) or of D(II): HKL is ('doubly') extinct (absent) in D(I) *as well as* in D(II).

It is of interest to present the relative frequencies of the four coincidence cases (i)–(iv) above as a function of the twin index m (see Table 1). Note the strong reduction of the coincidences (i) and the strong increase of the doubly extinct reflections (iv) with increasing index m. The latter extinct reflections (iv) are 'non-space-group extinctions'. These strange absences are an indication of the presence of twins by reticular merohedry and a help in determining the twin law.

[4] In some cases of reticular merohedral twins certain indices are *always integer*, *e.g.* for the tetragonal $\Sigma5$ and hexagonal $\Sigma7$ twins which preserve the tetragonal or hexagonal axis. Here the index l is *always integer* (*cf.* §§5 and 6).

Table 1
Relative frequencies of the four coincidence cases (i)–(iv) for the general Σm twins and the specific $\Sigma3$, $\Sigma5$ and $\Sigma7$ twins treated in this paper.

For each twin case the sum of all fractions is 1.

Coincidence cases	Σm	$\Sigma1$	$\Sigma3$	$\Sigma5$	$\Sigma7$
(i) Coincidence pair	$1/m^2$	1	1/9	1/25	1/49
(ii) Single reflections of domain D(I)	$(m-1)/m^2$	0	2/9	4/25	6/49
(iii) Single reflections of domain D(II)	$(m-1)/m^2$	0	2/9	4/25	6/49
(iv) Doubly extinct reflections	$(m-1)^2/m^2$	0	4/9	16/25	36/49

Note that these considerations apply only if the diffraction pattern is evaluated on the basis of the coincidence-site lattice providing integer reflection indices HKL for all coincidence cases (i)–(iv). A first indication of these 'non-space-group extinctions' was given by Buerger (1960, ch. 5).

In the present paper we deal only with twins by reticular merohedry which are possible for all lattice parameters of a crystal system, *i.e.* which are not due to an accidental special fit of the lattice parameters. These are twins that preserve the orientation of the three-, four- or sixfold symmetry axis, with a twin reflection plane m parallel or a twofold twin axis normal to the main axis [for rhombohedral crystals also with the twin plane m normal to the (odd) threefold axis]. In these cases the (partial) lattice coincidence is possible for *any value of c/a*. For cubic crystals these conditions apply to the preservation either of a fourfold symmetry axis (similar to the tetragonal $\Sigma5$ twins) or of a threefold axis. The latter case corresponds to the cubic spinel law and is treated in §4. There are only a few known cases of twinning by *exact reticular merohedry* ('exact' in contrast to only 'approximate' partial superposition of the lattices of the twin domains: twinning by '*reticular pseudo-symmetry*'). The most important twin cases are the following:

(*a*) Obverse/reverse $\Sigma3$ twins ('spinel twins') of *rhombohedral* and *cubic* crystals (*cf.* Hahn & Klapper, 2003, p. 406 & 407). These very frequent and important $\Sigma3$ twins are treated in detail in §§3 and 4 below.

(*b*) Twins of *cubic* crystals with any twin reflection plane $m'(hkl)$ or any twofold twin axis $2'[uvw]$. The twin index is $\Sigma = h^2 + k^2 + l^2$ or $\Sigma = \frac{1}{2}(h^2 + k^2 + l^2)$ and $\Sigma = u^2 + v^2 + w^2$ or $\Sigma = \frac{1}{2}(u^2 + v^2 + w^2)$, if the square sum is even (*cf.* Hahn & Klapper, 2003, pp. 417–419). A special case is the spinel twin with twin mirror plane $m'(111)$ and/or twofold twin axis $2'[111]$, case (*a*) above.

(*c*) Twins of tetragonal crystals with twin mirror planes of type $(hk0)$ or twofold twin axes $[uv0]$ and twin index $\Sigma = h^2 + k^2$ or $\Sigma = \frac{1}{2}(h^2 + k^2)$ and $\Sigma = u^2 + v^2$ or $\Sigma = \frac{1}{2}(u^2 + v^2)$. The smallest lattice index of this kind of twins, $\Sigma = 5$, is provided by twin mirror planes $m'(120)$ and $m'(310)$ or twofold twin axes $2'[2\bar{1}0]$ and $2'[\bar{1}30]$. Examples are given in §5 below.

(*d*) Twins of hexagonal crystals with twin mirror planes of type $m'(hk0)$ or twin axes $2'[uv0]$ and twin index

$\Sigma = h^2 + hk + k^2$ or $1/3(h^2 + hk + k^2)$ and $\Sigma = u^2 - uv + v^2$ or $1/3(u^2 - uv + v^2)$. The smallest lattice index, $\Sigma = 7$, is obtained for twin mirror planes $m'(12\bar{3}0)$ and $m'(\bar{5}410)$ or twofold twin axes $2'[\bar{2}10]$ and $2'[450]$. This case is treated in §6. A real example of this twin type, however, is not known.

2.2. X-ray intensities and face-form eigensymmetries

As shown above, the diffraction record of a crystal twinned by reticular merohedry contains coincident (superimposed) twin-related reflections [case (i) above] and single reflections [cases (ii) and (iii) above], the intensities of which may or may not be influenced by the twinning. The single reflections are *always* influenced by the twinning because the volume of the twin partner involved is only a fraction of the total twin volume. This allows one to determine the volume fractions of the two twin domains D(I) and D(II). The intensity features of the twin-related *superimposed* reflections (i) follow the same rules as given in the previous paper on Σ1 twins (Klapper & Hahn, 2010). For these superimposed reflections two cases may occur [*cf.* twin diffraction cases A and B in §1, (iii) above]:

(*a*) If the twin element belongs to the oriented *eigensymmetry* of the corresponding face form {*hkl*}, the structure-factor moduli of the twin-related superimposed reflections *hkl* and $h'k'l'$ are symmetrically equivalent under the point group of the crystal and thus are equal, even including anomalous scattering (twin diffraction case A). The intensities of these superimposed reflections are independent of the volume ratio of the twins.

(*b*) If the twin element does *not* belong to the oriented *eigensymmetry* of the face forms {*hkl*} and $\{h'k'l'\}$, the structure factors of the superimposed reflections *hkl* and $h'k'l'$ are *not* equivalent and, hence, their moduli are not equal (diffraction case B). These reflections are further subdivided into those with different geometric structure factors (diffraction case B1) and those forming Bijvoet sets (diffraction case B2).

Thus, for twins by reticular merohedry, with respect to diffraction intensities five groups of reflections are distinguished: superimposed equivalent reflections (*i.e.* not sensitive to the twin ratio, diffraction case A), superimposed non-equivalent reflections with different geometric structure-factor moduli (case B1), superimposed non-equivalent but 'opposite' reflections with different anomalous-scattering contributions (Bijvoet sets, case B2) [all of type (i) in Table 1] and non-superimposed ('single') reflections [types (ii) and (iii) in Table 1]. In addition, unusual 'non-space-group absences' occur [type (iv) in Table 1]. For non-symmorphic space groups these unusual absences may be even more complicated by regular extinctions due to unit-cell centring, screw axes and glide planes. This is discussed in §§3.5, 4.2, 5.4 and 6.4.

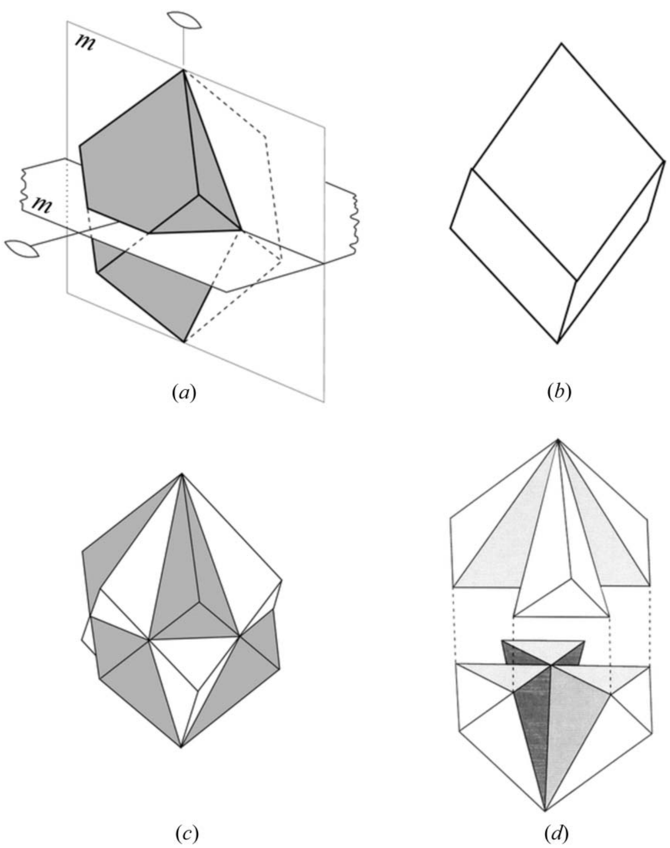

Figure 1
Twin intergrowth of 'obverse' and 'reverse' rhombohedra of rhombohedral $FeBO_3$ (point group $\bar{3}2/m$). (*a*) 'Obverse' rhombohedron with four of the 12 alternative twin elements. (*b*) 'Reverse' rhombohedron (twin orientation). (*c*) Interpenetration of both rhombohedra, as observed in penetration twins of $FeBO_3$. (*d*) Idealized skeleton of the six components (exploded along [001] for better recognition) of the 'obverse' orientation state shown in (*a*). The components are connected at the edges along the threefold and the twofold *eigensymmetry* axes. The shaded faces are $\{10\bar{1}0\}$ and (0001) coinciding twin reflection and contact planes with the twin components of the 'reverse' orientation state. Parts (*a*) to (*c*) courtesy of D. Götz *et al.* (2012); after Hahn & Klapper (2003, p. 406).

3. Obverse/reverse (spinel) Σ3 twins of rhombohedral crystals

3.1. General remarks on Σ3 twin laws

The obverse/reverse Σ3 twins of rhombohedral and cubic crystals, the latter usually called spinel twins, are by far the most frequent 'twins by reticular merohedry'.[5] Usually only *two* Σ3 twin laws are considered, one rotation twin with the twofold twin axis parallel to the threefold symmetry axis and one reflection twin with the twin reflection plane perpendicular to the threefold symmetry axis (both laws being identical for centrosymmetric point groups). Closer group-theoretical inspection, however, has revealed that there are *four* Σ3 obverse/reverse twin laws: one further twofold rotation twin 2[210] and one further reflection twin $m(10\bar{1}0)$, perpendicular to [210] (hexagonal axes).

All four twin laws are different (*i.e.* not 'alternative') only for the *rhombohedral* point group 3 (order 3), *i.e.* the *trigonal* point group 3 based on a *rhombohedral* lattice. For the

[5] The rhombohedral Σ3 twins treated here are 'twins by reticular merohedry with *parallel* threefold axes'. They are thus independent of the *c*/*a* ratio (hexagonal axes) or the rhombohedral angle α (rhombohedral axes) and can occur in any rhombohedral crystal. Twins 'with *inclined* threefold axes' depend on the axial ratio or on α. Both types have been derived by Grimmer (1989*b*).

rhombohedral groups $\bar{3}$, 32 and 3*m* (order 6) the two rotation and the two reflection twin laws merge in different ways into two twin laws each, and for point group $\bar{3}2/m$ all four twin laws coalesce into one. Details of these 11 $\Sigma3$ twin laws, their cosets (sets of alternative twin operations), their theoretical background and their relation to the merohedral $\Sigma1$ twin laws of the trigonal point groups are presented in Appendix *A*.

3.2. General remarks on rhombohedral and hexagonal coordinate axes

Rhombohedral crystals can be described by two coordinate systems (each in two settings, 'obverse' and 'reverse') as follows:

(*a*) 'Rhombohedral axes' ($a = b = c$, $\alpha = \beta = \gamma$) with a primitive rhombohedral unit cell and, hence, without any integral reflection conditions. The two settings of this coordinate system correspond to two different orientations of the rhombohedron with respect to the hexagonal unit cell.

(*b*) 'Hexagonal axes' ($a = b \neq c$, $\alpha = \beta = 90^\circ$, $\gamma = 120^\circ$) with the *R*-centred triple hexagonal cell. This cell can occur in two settings: 'obverse' setting with lattice points 0, 0, 0; 2/3, 1/3, 1/3; 1/3, 2/3, 2/3 and integral reflection condition $-h + k + l = 3N$, and 'reverse' setting with lattice points 0, 0, 0; 1/3, 2/3, 1/3; 2/3, 1/3, 2/3 and integral reflection condition $h - k + l = 3M$ (*N*, *M* integers).

The two settings are related either by a 180° rotation around the threefold symmetry axis, 2[111] (rhombohedral) or 2[001] (hexagonal) (*cf.* Fig. 1), preserving the handedness of the basis vectors, or by a reflection through the plane normal to the threefold axis, *m*(111) (rhombohedral) or *m*(0001) (hexagonal), reversing the handedness of the basis vectors. The basis-vector transformations between these settings are as follows ('obverse' basis vectors **a**, **b**, **c**, 'reverse' basis vectors **a**′, **b**′, **c**′):

Hexagonal axes:

$$\mathbf{a}' = -\mathbf{a},\quad \mathbf{b}' = -\mathbf{b},\quad \mathbf{c}' = +\mathbf{c}\quad (180^\circ \text{ rotation around } [001])$$
$$\mathbf{a}' = +\mathbf{a},\quad \mathbf{b}' = +\mathbf{b},\quad \mathbf{c}' = -\mathbf{c}\quad [\text{reflection across } m(0001)]$$

Rhombohedral axes:

$$\begin{array}{ll} \mathbf{a}' = +1/3(-\mathbf{a} + 2\mathbf{b} + 2\mathbf{c}) & \mathbf{a}' = -1/3(-\mathbf{a} + 2\mathbf{b} + 2\mathbf{c}) \\ \mathbf{b}' = +1/3(2\mathbf{a} - \mathbf{b} + 2\mathbf{c}) & \mathbf{b}' = -1/3(2\mathbf{a} - \mathbf{b} + 2\mathbf{c}) \\ \mathbf{c}' = +1/3(2\mathbf{a} + 2\mathbf{b} - \mathbf{c}) & \mathbf{c}' = -1/3(2\mathbf{a} + 2\mathbf{b} - \mathbf{c}) \\ (180^\circ \text{rotation around } [111]) & [\text{reflection across } m(111)]. \end{array}$$

These two transformations will be used in the subsequent section for the derivation of the $\Sigma3$ reverse/obverse twins. The transformations between the primitive rhombohedral cell and the triple hexagonal cell and *vice versa* are given by Arnold (2002) in Table 5.1.3.1 (p. 81) and Fig. 5.1.3.6 (p. 84).

3.3. Description of rhombohedral obverse/reverse twins by hexagonal axes

Spinel twins occur frequently in rhombohedral crystals with a calcite structure, for example as growth twins in calcite $CaCO_3$, iron borate $FeBO_3$ (Kotrbova *et al.*, 1985; Klapper, 1987), aluminium oxide Al_2O_3 (corundum, sapphire) (Wallace & White, 1967). The point group of these crystals is the (centrosymmetric) holohedral point group of the rhombohedral lattice $\bar{3}2/m$ (order 12), the twin composite symmetry is 6/*m*2/*m*2/*m* (order 24, supergroup of index [2]) and the twinning can be described by any of the 12 alternative twin operations of the coset (*cf.* Hahn & Klapper, 2003, p. 406), among which the following are the most illustrative ones: '*twofold axis* [001]', '*reflection plane* (0001)', '*twofold axis* [210]' and '*reflection plane* (10$\bar{1}$0)' (hexagonal axes), *cf.* Appendix *A*. These twin elements, each of which transforms an obverse into a reverse rhombohedron and *vice versa*, are shown in Fig. 1. The lattices of the two twin domains are only partially coincident and form a *twin lattice* (coincidence-site lattice) which is a (diluted) hexagonal sublattice of index $\Sigma = 3$. The reciprocal lattice of the twin is a hexagonal superlattice of index 3.

The face forms, the twin elements and the reflections modified or not modified by the twinning are independent of the description of the rhombohedral lattice by rhombohedral or hexagonal axes (*cf.* §3.2). An additional feature arises due to the partial $\Sigma3$ lattice coincidence: there occur two types of reflections, *superimposed* and *single*, which are determined by the (integral) reflection conditions of the obverse and reverse settings of the rhombohedral lattice (only if referred to hexagonal axes): $-h + k + l = 3N$ for the *obverse* and $h' - k' + l' = 3M$ (*N*, *M* integers) for the twin-related *reverse* setting. If a pair of twin-related reflections *hkil and h′k′i′l′* obeys both conditions simultaneously, both reflections are *superimposed*, either with equal or with different *F* moduli (depending upon whether the reflections are equivalent or not). If only one of these conditions is obeyed, only one of the two twin-related reflections is 'present', the other 'absent' ('*single*' reflection). If none of the conditions is obeyed for a *hkil*/*h′k′i′l′* pair, both reflections are 'absent' ('*doubly extinct*', *cf.* §2.1 and Table 1). The distribution of the coincidence cases 'superimposed', 'single' and 'doubly extinct' in reciprocal space is, assorted in layers normal to the threefold symmetry axis, presented in Table 2.

In *all* reciprocal-lattice planes with $l = 3M$ (this includes the plane $l = 0$) there occur *no single reflections*. There are twin-related coinciding (superimposed) *present* reflections of both domain states *and* reflections *absent* ('doubly extinct') in both states. In these 3*M* layers reflections *hkil*/*h′k′i′l′* with $-h + k$ and $h' - k' = 3N$ are *both present* and superimposed (diffraction case B1), whereas reflections with $-h + k \neq 3N$ are *absent* for both twin domains. Reciprocal-lattice planes with $l \neq 3M$ contain only *single* and '*doubly extinct*' reflections, but *no superimposed present* reflections *hkil*/*h′k′i′l′*.

In the following, the coincidence behaviour is differentiated with respect to the various types of twin-related reflection sets. This can be easily derived by consideration of the oriented *eigensymmetries* of the corresponding face forms (Table 3, for the *rhombohedral holohedry* $\bar{3}2/m$): the reflections are coincident (superimposed) if the twin element is part of the *eigensymmetry* of the corresponding face form, they are 'single' if it is not (except for the special values of *h*, *k*, *l* obeying the conditions of subcolumn 5 in Table 3). The spinel

Table 2
The three types of coincidences of two rhombohedral reciprocal lattices, related by a twin rotation of 180° around the common threefold symmetry axis or by a twin mirror plane normal to this axis: coincident reflections, coincident absences and 'single' reflections.

Both reciprocal lattices are referred to the *same coordinate system (obverse, domain I) with one hexagonal reflection condition* $-h + k + l = 3N$, *i.e.* they are treated as reflections $hkil$ (domain I) and $\overline{hki}l$ or $hki\overline{l}$ (domain II). The coincidence types are described in hexagonal axes (*a*) and rhombohedral axes (*b*). For 'rhombohedral axes' integer indices hkl and fractional indices h_f', k_f', l_f' are used which correspond to non-extinct and extinct indices $hkil$ in 'hexagonal axes'. Note that $h + k + l = h' + k' + l'$ for $2'[111]$ and $h + k + l = -(h' + k' + l')$ for $m'(111)$. This holds for integer as well as for fractional indices.

Reciprocal-lattice planes ⊥ threefold axis	Coincident non-extinct ($\lvert F\rvert \neq 0$) reflections	Coincident extinct ($\lvert F\rvert = 0$) reflections	'Single' reflections (coincidence of $\lvert F\rvert \neq 0$ with $\lvert F\rvert = 0$)
(*a*) Hexagonal axes			
$hkil$, $l = 3N$	$\left.\begin{matrix} hkil \\ \overline{hki}l \end{matrix}\right\} -h+k=3M$	$\left.\begin{matrix} hkil \\ \overline{hki}l \end{matrix}\right\} -h+k\neq 3M$	—
$hkil$, $l = 3N + 1$	—	$\left.\begin{matrix} hkil \\ \overline{hki}l \end{matrix}\right\} -h+k=3M$	$\left.\begin{matrix} hkil \\ \overline{hki}l \end{matrix}\right\} -h+k=3M\mp 1$†
$hkil$, $l = 3N + 2$	—	$\left.\begin{matrix} hkil \\ \overline{hki}l \end{matrix}\right\} -h+k=3M$	$\left.\begin{matrix} hkil \\ \overline{hki}l \end{matrix}\right\} -h+k=3M\mp 2$†
(*b*) Rhombohedral axes			
hkl, $h+k+l=3N$	$\left.\begin{matrix} hkl \\ h'k'l' \end{matrix}\right\} -h+k+l=3N$	—	—
hkl, $h+k+l=3N+1$	—	—	hkl: integer indices, h_f', k_f', l_f': fractional indices‡
hkl, $h+k+l=3N+2$	—	—	hkl: integer indices, h_f', k_f', l_f': fractional indices‡

† The minus sign defines the single reflections of domain I (obverse), the plus sign those of domain II (reverse). ‡ The fractional indices are $h_f' = -h + 2(3N + q)/3$, $k_f' = -k + 2(3N + q)/3$, $l_f' = -l + 2(3N + q)/3$ with $q = 1$ or 2.

Table 3
Obverse/reverse (spinel) $\Sigma 3$ twins of rhombohedral crystals with *holohedral point group* $\overline{3}2/m$: types of reflections in hexagonal and rhombohedral indices; corresponding face forms in the untwinned and the twin composite point group; conditions for coincidence (*i.e.* simultaneous non-extinction) of twin-related reflections.

Face forms (reflection sets) that are different in the untwinned and the composite symmetry are printed in bold face. The corresponding diffraction cases B1 and A [different and equal *F* moduli, see §1 point (iii)] are given in column 7. The entry 'S + B1' in column 7 indicates that these reflection sets are 'single' if the conditions of columns 5 and 6 are not fulfilled and 'coincident' (diffraction case B1) if the conditions are fulfilled.

Types of reflections†		Untwinned crystal	Spinel twin	Condition for coincidence ('doubly present') of both domain states		
Hexagonal axes	Rhombohedral axes	point group $\overline{3}2/m$	composite symmetry $6/m2/m2/m$‡	Hexagonal axes	Rhombohedral axes	Twin diffraction case
$hkil$	hkl	**Ditrigonal scalenohedron**	**Dihexagonal dipyramid**	$-h + k = 3N$ and $l = 3M$	$h + k + l = 3N$	S§ + B1
$h0\overline{h}l$	hhl	**Rhombohedron**	**Hexagonal dipyramid**	$h = 3N$ and $l = 3M$	$2h + l = 3N$	S§ + B1
$hh\overline{2h}l$	$hk(2k-h)$	Hexagonal dipyramid	Hexagonal dipyramid	Any value of h and $l = 3M$	Any value of h, k	A
$hki0$	$hk(\overline{h+k})$	Dihexagonal prism	Dihexagonal prism	$-h + k = 3N$	Any value of h, k	A
$h0\overline{h}0$	$hh\overline{2h}$	Hexagonal prism	Hexagonal prism	$h = 3N$	Any value of h	A
$hh\overline{2h}0$	$0h\overline{h}$	Hexagonal prism	Hexagonal prism	Any value of h	Any value of h	A
$000l$	hhh	Pinacoid	Pinacoid	$l = 3M$	Any value of h	A

† For full reflection sets see Table 10.1.2.2 in Hahn & Klapper (2002). ‡ For the hexagonal composite symmetry only 'hexagonal axes' apply. § These 'single' reflections can be considered as B1 diffraction cases with one of the two *F* moduli exactly zero.

twin elements belong to the *eigensymmetries* of forms $\{hh\overline{2h}l\}$, $\{hki0\}$, $\{h0\overline{h}0\}$, $\{hh\overline{2h}0\}$ and $\{000l\}$ (hexagonal axes, column 1), *i.e.* these forms are the same in the untwinned and the composite point group. The twin-related reflections of these types always either fulfil or do not fulfil *simultaneously* the obverse and reverse 'non-extinction' conditions given in column 5, *i.e.* they are either both 'doubly present' (superimposed) or 'doubly extinct'. For the holohedry $\overline{3}2/m$ (lattice symmetry) the *F* moduli of these twin-related superimposed reflections are *equal*, *i.e.* their intensities are *not affected* by the twinning (diffraction case A). Face forms $\{hkil\}$ and $\{h0\overline{h}l\}$, however, are *different* in the *untwinned* and the *composite* symmetry (bold print in Table 3) because the twin element is *not* part of the 'untwinned *eigensymmetry*'. The reflections of these forms are *single*, except for the special h, k, l combinations (which include all reflections of orders ± 3, ± 6 *etc.*) given

Table 4
The twin diffraction cases for the 11 obverse/reverse Σ3 twin laws of rhombohedral crystals: point group, hexagonal twin composite group, composite group in black–white notation and twin diffraction cases for all seven reflection types (*cf.* Table 9d of Klapper & Hahn, 2010).

The indices of each reflection type are given in Bravais–Miller indices *hkil* for 'hexagonal axes' and below as Miller indices *hkl* for 'rhombohedral axes'. The entries 'S + B1' in columns 4 and 5 indicate the presence of both sets of (first- and second-order) '*single*' reflections and sets of superimposed twin-related (third-order) '*doubly present*' reflections, whereby reflections with $h + k + l = 3N$ are 'coincident' and those with $h + k + l \neq 3N$ are 'single'. The other reflection types (columns 6–10) consist only of superimposed '*doubly present*' reflections (see §3.4).

Point group†	Composite group†	Composite group (black–white notation)	Twin diffraction cases for the seven different types of reflections (face forms), for both hexagonal and rhombohedral axes: $hkil$ / hkl	$h0\bar{h}l$ / hhl	$hh\overline{2h}l$ / $hk(2k-h)$	$hki0$ / $hk(\overline{h+k})$	$h0\bar{h}0$ / $hh\overline{2h}$	$hh\overline{2h}0$ / $0h\bar{h}$	$000l$ / hhh
3	6	$6'(3)$	S + B1	S + B1	B1	B2	B2	B2	A
	$\bar{6}$	$\bar{6}'(3) = 3/m'$	S + B1	S + B1	B1	A	A	A	B2
	312	$312'$	S + B1	S + B1	B2	B1	A	B2	B2
	$31m$	$31m'$	S + B1	S + B1	A	B1	B2	A	A
$\bar{3}$	$6/m$	$6'(3)/m'$	S + B1	S + B1	B1	A	A	A	A
	$\bar{3}12/m$	$\bar{3}12'/m'$	S + B1	S + B1	A	B1	A	A	A
32	622	$6'(3)22'$	S + B1	S + B1	B2	B2	A	B2	A
	$\bar{6}2m$	$\bar{6}'(3)2m'$	S + B1	S + B1	A	A	A	A	A
$3m$	$6mm$	$6'(3)mm'$	S + B1	S + B1	A	B2	B2	A	A
	$\bar{6}m2$	$\bar{6}'(3)m2'$	S + B1	S + B1	B2	A	A	A	B2
$\bar{3}2/m$	$6/m2/m2/m$	$6'(3)/m'2/m2'/m'$	S + B1	S + B1	A	A	A	A	A

† Details of the obverse/reverse Σ3 twin laws and their cosets are given in Appendix *A*.

in subcolumn 5 which are 'doubly present'. These special superimposed reflections are *not symmetrically equivalent* in the untwinned symmetry and thus have different *F* moduli, *i.e.* their intensities are affected by the twinning with diffraction case B1.

In a simplifying view one could consider the obverse/reverse twins of rhombohedral crystals *formally* as Σ1 merohedral twins with a hexagonal lattice and the 'single' reflections as the superposition of two twin-related reflections, one of which has an *F* modulus *exactly zero*. In this approach single reflections would appear as diffraction case B1 and two *absent* superimposed twin-related reflections formally as diffraction case A. This latter interpretation, however, is of no practical significance with respect to X-ray intensities.

3.4. Description of obverse/reverse twins by rhombohedral axes

In the rhombohedral reference system there are *no integral absences*. Thus we speak here only of '*single*' and '*superimposed*' reflections, *cf.* Table 2. As is shown in Fig. 1, the spinel twin law maps the obverse rhombohedron onto the reverse one and *vice versa*. This corresponds to the transformation of the obverse into the reverse rhombohedral coordinate system. The rhombohedral Miller indices $(hkl)_{\rm obv}$ of domain state D(I) are transformed into the twin-related indices $(h'k'l')_{\rm rev}$ of state D(II) and *vice versa* by:

$$\begin{array}{ll} \text{Rotation twin } 2[111] & \text{Reflection twin } m(111) \\ h' = 1/3(-h+2k+2l) & h' = -1/3(-h+2k+2l) \\ k' = 1/3(2h-k+2l) & k' = -1/3(2h-k+2l) \\ l' = 1/3(2h+2k-l) & l' = -1/3(2h+2k-l). \end{array}$$

With $h + k + l = m$ this is simplified to

$$\begin{array}{ll} h' = -h + 2m/3 & h' = h - 2m/3 \\ k' = -k + 2m/3 & k' = k - 2m/3 \\ l' = -l + 2m/3 & l' = l - 2m/3. \end{array}$$

These transformations are identical with their inverses D(II) → D(I). Thus, in rhombohedral axes, reflections *hkl* with $m = h + k + l = 3M$ are coincident (superimposed). All others, leading to fractional (non-existing) reflections $h'k'l'$, are single (S). It is immediately clear that for the rhombohedral holohedry $\bar{3}2/m$ reflections of the sets *hkl* (ditrigonal scalenohedron) and *hhl* (rhombohedron) are superimposed for $n = 3N$ (forming diffraction case B1) and single for $n \neq 3N$, whereas *all* reflections of the sets $hk(2k-h)$ (hexagonal dipyramid), $(hk\overline{h+k})$ (dihexagonal prism), $hh\overline{2h}$ (hexagonal prism), $0h\bar{h}$ (hexagonal prism) and *hhh* (pinacoid) are superimposed with their (non-zero) twin-related counterparts. For the rhombohedral holohedry these latter sets of superimposed reflections are symmetrically equivalent and thus are diffraction case A. For Σ3 twins of the rhombohedral merohedries $3m$, 32, $\bar{3}$ or 3, however, these occur also as B1 or B2 diffraction cases (see §3.5 and Table 4).

The twin diffraction characteristics of the seven reflection sets (face forms) of the rhombohedral holohedry $\bar{3}2/m$ are presented in Table 3 in the hexagonal as well as in the rhombohedral reference system.

3.5. Twin diffraction characteristics of rhombohedral crystals with merohedral symmetry

So far only the obverse/reverse twins of the rhombohedral holohedry $\bar{3}2/m$ have been considered. In this section, obverse/reverse twinning in the four rhombohedral merohedries $3m$, 32, $\bar{3}$ and 3 is treated only in hexagonal indices. Since these merohedries are also based on a rhombohedral lattice, the coincidence (superposition) features are the same as for the holohedry $\bar{3}2/m$ (Table 2 and columns 5 and 6 of Table 3). Similarly, since the *eigensymmetries* of the face forms $\{hkil\}$ and $\{h0\bar{h}l\}$[6] *do not contain* the twin element for any rhombohedral merohedry, the superimposed reflections of these sets are *always* diffraction case B1. In contrast to $\bar{3}2/m$, however, in the merohedries $3m$, 32, $\bar{3}$ and 3 the *eigensymmetries* of the special forms $\{hh\overline{2h}l\}$, $\{hki0\}$, $\{h0\bar{h}0\}$, $\{hh\overline{2h}0\}$ and $\{000l\}$ do or do *not* contain the twin element and thus may exhibit diffraction cases A, B1 or B2. The intensity features of twin-related reflections in all 11 possible $\Sigma3$ twins of crystals with a rhombohedral lattice are presented in Table 4. For the rhombohedral lattice in the 'hexagonal-axes description', however, the non-extinction conditions given in Table 3, column 5, have – in addition – to be taken into account. These have consequences only for the reflection sets $\{hkil\}$ and $\{h0\bar{h}l\}$, which – besides having superimposed reflections of diffraction case B1 – also contain 'single' reflections (S + B1).

Concerning the non-symmorphic space groups and their extinctions, there are only two rhombohedral groups with glide planes, $R3c$ and $R\bar{3}2/c$, and three twin laws (*cf.* Appendix *A* and Table 13):

$3m \rightarrow 6mm$, twin operation $2'[001]_{\rm hex}$ or $2'[111]_{\rm rh}$;

$3m \rightarrow \bar{6}2m$, twin operation $m'(0001)_{\rm hex}$ or $m'(111)_{\rm rh}$;

$\bar{3}\,2/m \rightarrow 6/m2/m2/m$, twin operation $2'[001]_{\rm hex} = m'(0001)_{\rm hex}$ or $2'[111]_{\rm rh} = m'[111]_{\rm rh}$.

With the *c*-glide reflection condition hhl, $l = 2n$ and the $\Sigma3$ coincidence condition $m = 2h + l = 3M$ the twin-related reflection sets are (rhombohedral coordinates, see reverse/obverse transformations in §3.4)

$\{hhl\} \leftrightarrow \{h'h'l'\} = \{-h + 2M, -h + 2M, -l + 2M\}$.

The twin-related coincident sets are of the same type and thus subject to the same reflection condition $l = 2n$ and $l' = -l + 2M = -2(n - M)$, also even, *i.e.* 'non-extinct ↔ non-extinct' and, for $l = l' = 2n + 1$, 'extinct ↔ extinct'. The case 'extinct ↔ non-extinct' does not occur.

3.6. Structure determination of obverse/reverse (spinel) twins of rhombohedral crystals

In contrast to structure determinations of $\Sigma1$ twins (*cf.* Klapper & Hahn, 2010, §3.2), for rhombohedral $\Sigma3$ spinel twins some particular diffraction features have to be taken into account. If single-crystal intensity data are collected in rhombohedral indices based only on the obverse coordinate system, the data set contains *single* reflections of, say, domain I and superimposed reflections of domains I and II. The data set is incomplete because the single reflections of domain II are missing. Thus an (at least partial) data collection in the reverse setting is advisable. These data now contain the single reflections of domain II and again the superimposed reflections of domains I and II. The comparison of the intensities of the 'single obverse' and 'single reverse' data allows the determination of the volume ratio of domains I and II.

The same happens for the data collection in the hexagonal coordinate system if the *R* absences ($-h + k + l \neq 3M$ for the obverse, $h - k + l \neq 3N$ for the reverse setting) are taken into account and excluded from the data collection. In this case it is advisable to collect the intensity data without regard to any *R* absences. This data set contains the single reflections of domains I and II as well as the superimposed ones of both domains. It also contains the ('doubly coincident') systematic absences due to the *simultaneous occurrence* of the two *R* extinction conditions. These 'strange' absences are characteristic of the twin law and can be used for its determination.

Modern computer programs permit the determination of crystal structures from the complete diffraction data of twinned crystals, provided the twin law has been recognized before. A program for the refinement of twin structures is contained in the program package *SHELXL97* (Sheldrick, 1997, 2008; Herbst-Irmer & Sheldrick, 1998). Other programs for handling the diffraction data of twinned crystals are *TWINXLI* (Hahn & Massa, 1997) and *GEMINI* (Bruker, 2005). The power of the program *SHELXL* for the refinement of obverse/reverse $\Sigma3$ twins of rhombohedral crystals is demonstrated by Herbst-Irmer & Sheldrick (2002) for two complicated structures (space groups $R3c$ and $R3$, the latter combined with a $\Sigma1$ merohedral twin) and by Herbst-Irmer (2006) in the monograph '*Crystal Structure Refinement*'. Other examples are the structure determinations of obverse/reverse twins of the aluminosilicate zeolite chabazite K by Yakubovich *et al.* (2005), using *SHELXL97* and *TWINXLI*, and of $Ba_8Ru_{3.33}Ta_{1.67}O_{18}Cl_2$ by Wilkens & Müller-Buschbaum (1992), all with space group $R\bar{3}m$. The latter is of particular interest because structure determination and refinement were successfully carried out using *only* the single reflections of the larger domain, disregarding the overlapping reflections and the reflections of the other domain. This indicates that in suitable cases the structure of obverse/reverse twins can be determined without particular twinning software. An example of the use of *GEMINI* is the structure determination of a $\Sigma3$ twin of $(NaLa_2)NaPtO_6$ (space group $R\bar{3}c$) by Davies *et al.* (2003, especially 'Supplementary material'). Further $\Sigma3$ structure determinations are quoted in Appendix *A*. A survey of structure determination and refinement of obverse/reverse twins is given by Herbst-Irmer (2006).

3.7. X-ray diffraction topography of obverse/reverse twins

Similar to the various kinds of $\Sigma1$ twins, obverse/reverse $\Sigma3$ twin domains cannot be visualized by optical birefringence.[7] Usually these twins are recognized by their typical external morphology (*e.g.* re-entrant edges) and etch features of the

[6] They are the same as those in Table 9, subtable (c) of Klapper & Hahn (2010) for crystals with hexagonal lattices and $\Sigma1$ twin laws 2[001] and $m(0001)$. This is due to the fact that face forms are independent of the lattice type (hexagonal or rhombohedral).

[7] In principle, however, domains of $\Sigma3$ obverse/reverse reflection twins with twin laws $3 \rightarrow 3m$, $3 \rightarrow \bar{6} \equiv 3/m$ and $32 \rightarrow \bar{6}2m$ can be studied by the reversal of their optical rotation sense. The same applies to the corresponding trigonal $\Sigma1$ twins.

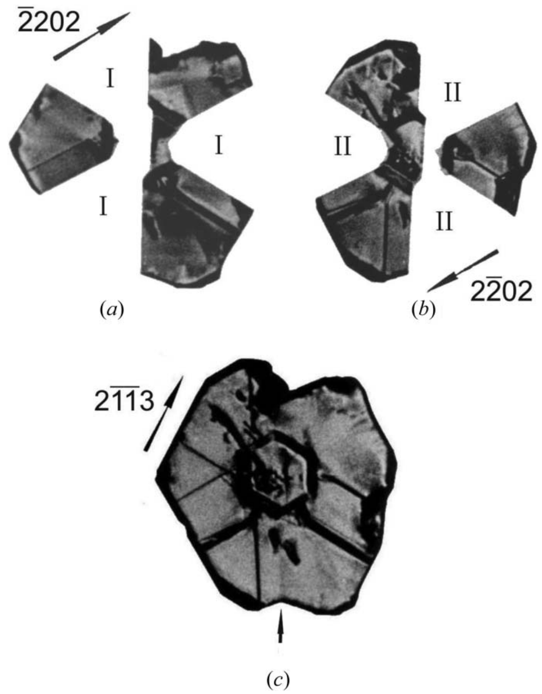

Figure 2
X-ray topographs (Mo $K\alpha_1$ radiation) of an obverse/reverse growth twin of $FeBO_3$ (calcite structure, space group $R\bar{3}m$), grown from the vapour phase by chemical transport. (0001) plate (diameter about 3.5 mm, thickness 0.2 mm), cut close to the centre of the crystal. (*a*) 'Single' reflection $\{\bar{2}202\}$ (rhombohedron) of obverse domain I (domain II 'extinct'); (*b*) 'single' reflection $\{2\bar{2}02\}$ (rhombohedron) of domain II (domain I 'extinct'); (*c*) coincident reflection $\{2\bar{1}\bar{1}3\}$ (hexagonal dipyramid) with equal *F* moduli of domains I and II (no domain contrast, diffraction case A). Arrows: diffraction vectors. In (*a*) and (*b*) the domains appear by 'black-and-white' contrast. The dark contrasts in the domains result from crystal defects. The straight contrast lines are dislocations or dislocation bundles. Note that the twin boundaries do not show diffraction contrast (except for a very faint contrast ending on the re-entrant corner marked by a small arrow in (*c*), indicating a good structural fit of the domains along their boundaries. The hexagonal contrast feature in the centre of (*c*) results from the growth-sector boundaries between the (0001) pinacoid and the $\{1\bar{1}01\}$ rhombohedral growth faces. Courtesy of D. Götz *et al.* (2012).

surface, but this does not yield information about the internal arrangement of the domains and twin boundaries. X-ray topography, however, is a very powerful method to study these domains and their distribution in a crystal. The most suitable reflections for imaging the domains are those for which one of the two twin-related reflections is extinct ($|F| = 0$), *e.g.* reflections which do not simultaneously obey the *R* non-extinction condition. An example is shown by the topographs of a (0001) plate [or (111) in rhombohedral axes] of $FeBO_3$ (calcite structure, space group $R\bar{3}2/c$, Figs. 2*a* and 2*b*). Using a reflection coincident with both twin-related counterparts provides a full image of both domains (Fig. 2*c*).

Obverse/reverse twins of the following crystals have been studied by *conventional X-ray topography* (Lang technique; Lang, 1999): corundum Al_2O_3, space group $R\bar{3}2/c$ (Wallace & White, 1967), and $FeBO_3$, space group $R\bar{3}2/c$ (Kotrbova *et al.*, 1985; Klapper, 1987, pp. 390–393; Götz *et al.*, 2012). In all these cases the obverse/reverse twin domains were visualized by black-and-white contrast using extinct/non-extinct twin-related reflections.

A study of the obverse/reverse $\Sigma3$ growth twinning of the laser crystal $Nd_xGd_{1-x}Al_3(BO_3)_4$ (space group *R*32) by *white-beam synchrotron radiation topography* is reported by Hu *et al.* (1998). In this case a special diffraction feature of twin-related reflections occurs: owing to the strong continuous-wavelength spectrum of the synchrotron source, besides the first-order reflection the higher-reflection orders (higher harmonics) are also generated, *i.e.* the first-order *hkl* with wavelength λ, the second-order $2h2k2l$ with $\lambda/2$, the third-order $3h3k3l$ with $\lambda/3$, all being superimposed onto the same Laue topograph. This is shown for a topograph recorded in first- and higher-order reflections $N(0.\bar{1}.1.5)$ in Fig. 4(*b*) of Hu *et al.* (1998). For the first- and second-order reflections $0.\bar{1}.1.5$ and $0.\bar{2}.2.10$ only the reverse domain fulfils the reflection condition $h - k + l = 3N$ (here $N = 2$ and 4) and is imaged, whereas the obverse domain is 'extinct' ($|F| = 0$, single reflection). Both reverse and obverse reflection conditions are simultaneously fulfilled for the third order $0.\bar{3}.3.15$ ($N = 6$, diffraction case B1). Thus, in the Laue topograph of superposed harmonic reflections $N(0.\bar{1}.1.5)$ the obverse domain appears with (comparatively) faint intensity.

4. Spinel $\Sigma3$ twins of cubic crystals

The term 'spinel twin' has been coined in mineralogy because of the frequent occurrence of this twinning in natural cubic spinels. There are four different twin laws, two of them represented by the well known twin elements 2[111] and *m*(111) and the other two by $2[2\bar{1}\bar{1}]$ and $m(2\bar{1}\bar{1})$. These four twin laws, their cosets and their combinations in the five cubic point groups are described in detail in Appendix *A* and Table 5.

Spinel twins of cubic crystals are $\Sigma3$ twins of the same type as the obverse/reverse twins of rhombohedral crystals described in §3 and illustrated in Fig. 1, but with the following differences: the lattice symmetry of the (untwinned) single crystal is the cubic holohedry $4/m\bar{3}2/m$ instead of $\bar{3}2/m$, and the rhombohedral angle α is, because of symmetry, exactly 90°. There are four threefold axes $\langle 111\rangle$ and four planes $\{111\}$ and, correspondingly, four sets of axes $\langle 2\bar{1}\bar{1}\rangle$ and planes $m\{2\bar{1}\bar{1}\}$ which can act as twin elements. Spinel twins mostly occur with twin elements related to only one of the threefold axes $\langle 111\rangle$, but combinations of twin elements related to two or more $\langle 111\rangle$ axes have also been observed, forming rather complicated twin aggregates (multiple and high-order twins; Hahn & Klapper, 2003, pp. 398 and 419). In the following we consider only twins with the twin elements 2[111], *m*(111), $2[2\bar{1}\bar{1}]$ and/or $m(2\bar{1}\bar{1})$.

Spinel twins frequently occur in crystals of the spinel ($MgAl_2O_4$) type, cubic metals and alloys (*cf.* Hahn & Klapper, 2003, pp. 407 and 419, and references therein), diamond (*e.g.* Yacoot *et al.*, 1998; Machado *et al.*, 1998), Si and Ge, compound semiconductors with the sphalerite ('zinc blende') structure (ZnS, GaAs, InP *etc.*), calcium fluoride CaF_2 and in some crystals with NaCl structure. Among the latter, crystals

Table 5
Twin intersection and hexagonal twin composite groups of the 11 possible [111] Σ3 cubic spinel twins.

For the details of the four Σ3 twin laws see Appendix *A*. For the twin composite groups in black–white notation see Table 4.

Untwinned cubic point group	Rhombohedral twin intersection group (index [4])	Twin law representatives (cubic axes)	Hexagonal twin composite group
23	3	2[111]	6
		m(111)	$\bar{6}$
		2[2$\bar{1}\bar{1}$]	312
		m(2$\bar{1}\bar{1}$)	31m
2/$m\bar{3}$	$\bar{3}$	2[111] + m(111)	6/m
		2[2$\bar{1}\bar{1}$] + m(1$\bar{1}\bar{1}$)	$\bar{3}$12/m
432	32	2[111] + 2[2$\bar{1}\bar{1}$]	622
		m(111) + m(2$\bar{1}\bar{1}$)	$\bar{6}$2m
$\bar{4}$3m	3m	2[111] + m(2$\bar{1}\bar{1}$)	6mm
		m(111) + 2[2$\bar{1}\bar{1}$]	$\bar{6}m$2
4/$m\bar{3}$2/m	$\bar{3}$2/m	2[111] + m(111) + 2[2$\bar{1}\bar{1}$] + m(2$\bar{1}\bar{1}$)	6/m2/m2/m

of the photographic materials AgCl and AgBr, precipitated from aqueous solutions, very frequently exhibit multiple Σ3 twins (Bögels *et al.*, 1999). The non-centrosymmetric crystals with sphalerite structure (point group $\bar{4}3m$) usually form twins with twin law 2[111], which preserves the direction of the polar [111] axis.

4.1. Splitting of cubic into rhombohedral face forms (reflection sets)

The *cubic* spinel Σ3 twin laws lead to *rhombohedral* intersection symmetries and hexagonal reduced twin composite symmetries (*cf.* Table 5). As a consequence, the twins must be described and treated in the maximal rhombohedral subgroup of their cubic point group, which is always of index 4 (*cf.* Fig. 10.1.3.2 on p. 796 of Hahn & Klapper, 2002). There are thus four conjugate rhombohedral point groups of the same type but different orientation, along the cubic directions [111], [$\bar{1}$11], [1$\bar{1}$1] and [11$\bar{1}$].

This group–subgroup decomposition of index [4] entails a ‘splitting’ into (up to four) rhombohedral face forms and/or a reduction of the cubic site (face) symmetries (again by a factor up to four). As a first example, the general form $\{hkl\}_{\rm cub}$ with site symmetry 1 of the cubic holohedry $4/m\bar{3}2/m$ (order 48) is considered. It splits into four rhombohedral forms $\{hkl\}_{\rm rh}$, $\{h\overline{kl}\}_{\rm rh}$, $\{\bar{h}k\bar{l}\}_{\rm rh}$ and $\{\overline{hk}l\}_{\rm rh}$, each with site symmetry 1, of the rhombohedral subgroup $\bar{3}2/m$ (order 12). These forms are related to the ‘starting set’ $\{hkl\}_{\rm rh}$ by the identity and the twofold cubic axes along $[100]_{\rm cub}$, $[010]_{\rm cub}$ and $[001]_{\rm cub}$. The complete $\{hkl\}$ sets of the five cubic and the five rhombohedral general forms can be found on pp. 776–782 and 786–790 of Hahn & Klapper (2002).

Furthermore, the general face forms of the rhombohedral subgroups appear as one ‘basic’ and up to four ‘limiting’ forms, depending on the special values of the Miller indices h, k, l. Thus the cubic hexakisoctahedron $\{123\}_{\rm cub}$ (48 faces) is split into four rhombohedral forms $\{123\}_{\rm rh}$ (hexagonal bipyramid with $h + k + l = 3k$), $\{\overline{12}3\}_{\rm rh}$ (dihexagonal prism with $h + k + l = 0$), $\{\bar{1}2\bar{3}\}_{\rm rh}$ (ditrigonal scalenohedron) and $\{1\overline{23}\}_{\rm rh}$ (ditrigonal scalenohedron), each with 12 faces, as shown in Fig. 3.

As a second example, the cube $\{h00\}_{\rm cub}$ (six faces) with face symmetry $4mm$ (order 8) in point group $4/m\bar{3}2/m$ is not split, but occurs in $\bar{3}2/m$ as four coincident 90° rhombohedra $\{h00\}_{\rm rh}$ with the reduced face symmetry m (order 2), *i.e.* the ‘splitting’ is due to a reduction of the face symmetry by a factor 4. The coincidence of these four split forms is due to the *eigensymmetry* of the 90° rhombohedron, which contains the three twofold axes ⟨100⟩ of the cubic supergroup. All other splitting cases are in between these two examples, as shown in Table 6.

The ‘subgroup splitting’ of the cubic forms is explained in detail in Appendix *B*, together with a complete list of all split forms of the five cubic point groups (Table 15). It should be emphasized that the ‘subgroup splitting’ explained above and

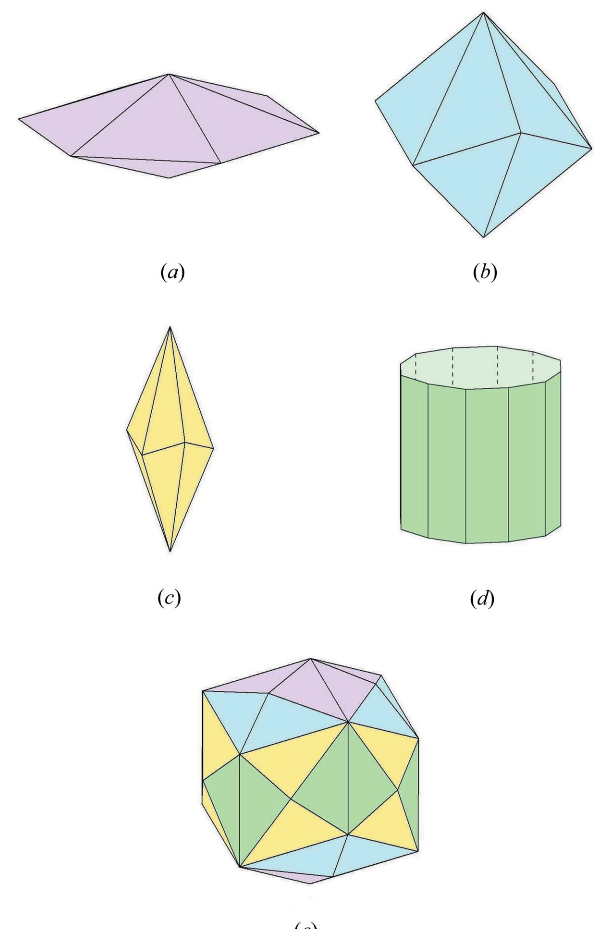

Figure 3
Splitting of the cubic face form $\{123\}_{\rm cub}$ (hexakisoctahedron, point group $4/m\bar{3}2/m$, 48 faces) into four rhombohedral subforms (12 faces each) of point group $\bar{3}2/m$ with their rhombohedral axes along $[111]_{\rm cub}$ and rhombohedral angle α = 90° (*cf.* Appendix *B*). (*a*) $\{123\}_{\rm rh}$ (hexagonal dipyramid), (*b*) $\{\bar{1}23\}_{\rm rh}$ (ditrigonal scalenohedron), (*c*) $\{1\bar{2}3\}_{\rm rh}$ (ditrigonal scalenohedron) and (*d*) $\{12\bar{3}\}_{\rm rh}$ (dihexagonal prism), (*e*) combination of these forms yields the cubic hexakisoctahedron. [Note that the central distances of the faces are different for the four rhombohedral forms, but equal in the combination (*e*).]

Table 6
Spinel [111] twins in the cubic holohedry $4/m\overline{3}2/m$: types of reflections with multiplicity and coincidence conditions in parentheses, corresponding rhombohedral subface forms in the twin intersection and the reduced twin composite point groups with number of faces, and twin diffraction cases.

Face forms (reflection sets) that are different in the intersection and the composite symmetry are printed in bold. In column 4 'S' refers to 'single' reflections for $n = h + k + l \neq 3N$, 'B1' to coincident reflections for $n = h + k + l = 3N$. Note that in this centrosymmetric group the four spinel twin elements form *one* twin law (*cf.* Appendix *A* and Table 5).

Face forms (types of reflections) in point group $4/m\overline{3}2/m$ (untwinned, *P* lattice)†	Subface forms in intersection group $\overline{3}2/m$ along [111]	Subface forms in reduced composite group $6/m2/m2/m$‡	Twin diffraction case
$\{hkl\}$ (48) ($n = h + k + l = 3N$)	**Ditrigonal scalenohedron (12)**	**Dihexagonal dipyramid (24)**	S + B1
$\{hk(2k-h)\}$ ($n = 3k$)	Hexagonal dipyramid (12)	Hexagonal dipyramid (12)	A
$\{hk(\overline{h+k})\}$ ($n = 0$)	Dihexagonal prism (12)	Dihexagonal prism (12)	A
$\{hhl\}$ (24) ($2h + l = 3N$)	**Rhombohedron (6)**	**Hexagonal dipyramid (12)**	S + B1
$\{hh\,\overline{2h}\}$ ($n = 0$)	Hexagonal prism (6)	Hexagonal prism (6)	A
$\{0kl\}$ (24) ($k + l = 3N$)	**Ditrigonal scalenohedron (12)**	**Dihexagonal dipryamid (24)**	S + B1
$\{0k2k\}$ ($n = 3N$)	Hexagonal dipyramid (12)	Hexagonal dipyramid (12)	A
$\{0kk\}$ (12) ($k = 3N$)	**120° rhombohedron (6)**	**Hexagonal dipyramid (12)**	S + B1
$(0k\overline{k})$ (k any integer value)	Hexagonal prism (6)	Hexagonal prism (6)	A
$\{hhh\}$ (8) (h any integer value)	Pinacoid (2)	Pinacoid (2)	A
$\{hh\overline{h}\}$ ($h = 3N$)	**60° rhombohedron (6)**	**Hexagonal dipyramid (12)**	S + B1
$\{h00\}$ (6) ($h = 3N$)	**90° rhombohedron (6)**	**Hexagonal dipyramid (12)**	S + B1

† The various face forms, coincidence features and diffraction cases are the same for the cubic primitive (*P*), body-centred (*I*) and face-centred (*F*) lattices (see text). For the *I* and *F* centrings, however, their reflection conditions ($h + k + l = 2N$ for *I* and all h, k, l either even or odd for *F*) have to be additionally taken into account. ‡ For the hexagonal composite symmetry only 'hexagonal axes' apply.

in Appendix *B* is a pure group–subgroup problem, independent of any application such as twinning, phase transitions or crystal morphology.

4.2. Cubic Σ3 twins and their diffraction cases

The 11 Σ3 twin laws and their applications to cubic crystals are very similar to those of rhombohedral crystals (*cf.* §3.1, Appendix *A* and Table 5).

With respect to face forms (reflection sets), the spinel twinning of cubic crystals of any cubic point group exhibits the following features:

(*a*) There is no cubic face form $\{hkl\}_{\rm cub}$ which is *completely* mapped onto itself by a spinel-twin operation, *i.e.* no Σ3 twin element is an *eigensymmetry* element of any cubic face form.

(*b*) The (up to four) rhombohedral subforms (reflection sets) of one and the same cubic form usually exhibit different twin diffraction cases S + B1, B1, B2 or A, depending on the twin law, although all faces of the subforms are symmetrically equivalent in the cubic supergroup and have equal *F* moduli. This is illustrated in Table 7 for the split forms of the cubic form $\{123\}_{\rm cub}$ in point groups $4/m\overline{3}2/m \rightarrow \overline{3}2/m$ (*cf.* Fig. 3), 432 → 32 and $\overline{4}3m \rightarrow 3m$. Another illustration of the different diffraction cases of split forms is given for the centrosymmetric rhomb-dodecahedron $\{0kk\}_{\rm cub}$, which occurs in all cubic groups, in Table 14 of Appendix *B*.

(*c*) A special feature occurs for those cubic forms which are *centrosymmetric* in the *non-centrosymmetric* cubic point groups 432, $\overline{4}3m$ and 23, *e.g.* forms $\{0kk\}_{\rm cub}$ (rhomb-dodecahedron) and $\{h00\}_{\rm cub}$ (cube). These split into pairs of 'opposite' (morphologically inverted) rhombohedral subforms. For some twin laws the two opposite forms of a pair are mapped upon each other, thus forming B2 diffraction cases, because they are – formally – *not equivalent* in the rhombohedral subgroup. In the cubic supergroup, however, they are *equivalent*, have equal *F* moduli and thus provide in reality diffraction case A. This particular diffraction case is denoted as $\underline{\rm A}$. It is discussed in detail in Appendix *B* and especially in Table 14.

Thus, the various 'rhombohedral' subsets $\{hkl\}_{\rm rh}$ of a cubic reflection set $\{hkl\}_{\rm cub}$ exhibit, despite being 'cubically'

Table 7
Diffraction cases of the rhombohedral subforms $\{123\}_{\rm rh}$ [$n = 6 = 3k$, (bi)pyramids] $\{\overline{1}\overline{2}3\}_{\rm rh}$ ($n = 0$, prisms), $\{1\overline{2}\overline{3}\}_{\rm rh}$ ($n = -2$, scalenohedra/trapezohedra/ditrigonal pyramids) and $\{12\overline{3}\}_{\rm rh}$ ($n = -4$, scalenohedra/trapezohedra/ditrigonal pyramids) of the cubic face form $\{123\}_{\rm cub}$ for the Σ3 twin laws $2[111]_{\rm cub}$ and $m(111)_{\rm cub}$ of the cubic groups $4/m\overline{3}2/m$, 432 and $\overline{4}3m$.

Group→subgroup	Rhombohedral split forms of $\{123\}_{\rm cub}$	Twin diffraction case $2[111]_{\rm cub}$	Twin diffraction case $m(111)_{\rm cub}$
$4/m\overline{3}2/m \rightarrow \overline{3}2/m$ (*cf.* Fig. 3)	1 hexagonal bipyramid	A	A
	1 dihexagonal prism	A	A
	2 ditrigonal scalenohedra	S + B1	S + B1
432→32	1 trigonal bipyramid	B2	A
	1 ditrigonal prism	B2	A
	2 trigonal trapezohedra	S + B1	S + B1
$\overline{4}3m \rightarrow 3m$	1 hexagonal pyramid	A	B2
	1 ditrigonal prism	B2	A
	2 ditrigonal pyramids	S + B1	S + B1

symmetry equivalent, quite different intensity relations of twin-related reflections. The subsets $\{hkl\}_{\rm rh}$ follow exactly the rules given in §3 for the obverse/reverse twins of rhombohedral crystals described in 'rhombohedral axes'. In particular, the index transformations given in §3.4 are also valid for the subset relation $\{hkl\} \rightarrow \{h'k'l'\}$ in the spinel twins of cubic crystals.

The above coincidence and intensity features of twin-related reflection sets, derived so far for cubic P lattices (α = 90°), are also valid for I- and F-centred cubic lattices, *i.e.* the twin operation maps non-extinct reflections of domain state D(I) upon non-extinct reflections of domain state D(II) and *vice versa*. This is due to the fact that both the I- and the F-centred cubic lattices can be based on (primitive) rhombohedral lattices [rhombohedral angle $\alpha = 180° - \arccos(1/3) = 109.47°$ for I and $\alpha = \arccos(1/2) = 60°$ for F] with the threefold axes of both domains along the cube diagonal [111], and that the coincidence and diffraction cases of the diffraction record do not depend on the chosen reference system and the value of the rhombohedral angle α.

Combining the $\Sigma3$ coincidence condition $h + k + l = 3n$ with the reflection conditions of the I lattice ($h + k + l = 2m$) and the F lattice (h, k, l all odd or even), the following conditions for the coincidence of twin-related non-extinct reflection sets are obtained:

I lattice:

$$h + k + l = 3 \times 2m = 6m,$$

F lattice:

$$\begin{aligned} h + k + l &= 3(2m \pm 1) = 6m \pm 3 \text{ for all } h, k, l \text{ odd} \\ &= 3 \times 2m = 6m \text{ for all } h, k, l \text{ even.} \end{aligned}$$

Space-group absences (glide planes, screw axes) of non-symmorphic space groups may lead to extinct↔non-extinct coincidences of $\Sigma3$-related reflection sets. Since the list of these cases is rather long, only a few illustrative examples are given.

(i) Space group $P2_1/a\overline{3}$, reflection set $\{0kl\}$ (pentagon dodecahedron), reflection condition $k = 2n$. $\Sigma3$ coincidence condition $k + l = 3m$ (plus cyclic permutations). Applying the reverse/obverse transformation (§3.4) provides:

$\{0kl\} \leftrightarrow \{h'k'l'\} = \{2m, -k + 2m, -l + 2m\}$.

For $m \neq 0$ the $\{0kl\}$ sets coincide with sets of type $\{h'k'l'\}$ which are not subject to the a-glide extinction, *i.e.* there are $\Sigma3$ coincidences of extinct and non-extinct reflection sets for $k = 3(2N \pm 1) = 6N \pm 3$ and non-extinct on non-extinct ones for $k = 6N$. Similarly for diffraction set $\{h00\}$ (cube): $h = 3(2N \pm 1)$ and $h = 6N$, respectively.

(ii) Space group $P2_1/n\overline{3}$, reflection sets $\{0kl\}$ (pentagon dodecahedron) and $\{h00\}$ (cube), reflection conditions $k + l = 2n$ and $h = 2n$ (plus cyclic permutations). This corresponds to the I-lattice reflection condition: $k + l = 6N$ and $h = 6N$ for non-extinct↔non-extinct pairs and $k + l = 6N \pm 3$ and $h = 6N \pm 3$ for extinct↔non-extinct pairs.

(iii) Space groups with 2_1 and 4_2 screw axes along [100], reflection sets $\{h00\}$ (plus cyclic permutations). The reflection condition $h00$: $h = 2n$ leads for $h = 6N$ to non-extinct↔non-extinct coincidence pairs, for $h = 6N \pm 3$ to extinct↔non-extinct pairs. For 4_1 and 4_3 screw axes with $h00$: $h = 4n$, non-extinct↔non-extinct pairs occur for $h = 12N$, extinct↔non-extinct pairs for all $h = 12N \pm 4$.

In cubic space groups only reflection sets of type $\{hhl\}$, $\{0kl\}$ and $\{h00\}$ may be subject to space-group extinctions. The above superposition of non-extinct with non-extinct or with extinct sets is also valid for their rhombohedral subforms, which always exhibit diffraction case S + B1 (see Table 15, bold print in lines 4, 6, 10). Here the extinct↔non-extinct superposition is also a B1 diffraction case with one $|F| = 0$.

A particular situation arises for the special reflection sets $\{hh2h\}_{\rm cub}$, $\{0k2k\}_{\rm cub}$ and $\{0kk\}_{\rm cub}$ which may also exhibit space-group extinctions and contain the rhombohedral subsets $\{hh\overline{2h}\}_{\rm rh}$ (n = 0, prisms), $\{0k2k\}_{\rm rh}$ ($n = 3k$, pyramids) and $\{0k\overline{k}\}_{\rm rh}$ (n = 0, prisms), respectively (see Table 15, lines 5, 7 and 8, subsets in normal print). These subsets completely coincide with their $\Sigma3$-twin counterparts (no singles) and are either symmetrically equivalent or 'Bijvoet related' and, thus, provide either A or B2 diffraction cases. Twin-related reflection subsets of this kind with space-group extinctions provide extinct↔extinct and non-extinct↔non-extinct pairs, but no extinct↔non-extinct pairs.

The splitting of cubic into rhombohedral face forms and the twin diffraction cases for all rhombohedral subsets and for all $\Sigma3$ spinel twin laws in the five cubic point groups are included in Table 15 of Appendix *B*, together with remarks providing more detailed information.

4.3. X-ray diffraction topography of cubic spinel twins

Cubic spinel twins have so far been observed only in crystals with well known structures (metals, spinels, crystals with diamond, sphalerite and NaCl structure). Thus, there exist no structure determinations of spinel-twinned cubic crystals. Conventional X-ray topography and white-beam synchrotron topography, however, have quite often been applied to depict the distribution of twin domains and twin boundaries within the crystal. Examples are the studies of diamond (Machado *et al.*, 1998; Yacoot *et al.*, 1998; Fritsch *et al.*, 2005; Moore, 2009), III–V and II–VI compound semiconductors (sphalerite structure) InP (Tohno & Katsui, 1986) and CdTe (Buck & Nagel, 1981), and natural spinels (Fregola *et al.*, 2005; Fregola & Scandale, 2007). In all these cases the twin domains were visualized by black-and-white contrast of non-extinct/extinct twin-related reflections. In some synchroton-radiation studies domains 'extinct' in first- and second-order reflections ($|F| = 0$) were depicted in the corresponding 'non-extinct' third-order reflection ($|F| \neq 0$, *cf.* §3.7).

5. $\Sigma5$ twins of tetragonal crystals

In this section *tetragonal* 'twins by reticular merohedry with parallel c axes' are treated. The smallest possible twin lattice index is $\Sigma = h^2 + k^2 = 5$ for a (120) reflection twin. These $\Sigma 5$ twins are very rare, only a few cases are known (see references below). Tetragonal twins of higher lattice index [*e.g.* $\Sigma 13$ for (230) or $\Sigma 17$ for (140) reflection twins] are not known.

The $\Sigma 5$ twins considered here do not depend on the tetragonal axial ratio *c*/*a*, *i.e.* they are, in principle, possible in any tetragonal crystal. This is due to the *parallelism* of the tetragonal *c* axes of the twin partners and their coincidence lattice ('parallel *c*-axis twins'). Since the twin operation preserves the tetragonal *c* axis, the twinning is a two-dimensional phenomenon, *i.e.* the distribution of coincident, single and extinct reflections is the same for all reciprocal layers $hk0$, $hk\pm1$, $hk\pm2$ *etc*. This holds for all tetragonal point groups. In contrast to 'parallel *c*-axis twins', twins by reticular merohedry with *inclined c* axes are only possible for special tetragonal c/a ratios. Possible theoretical cases have been derived and listed by Grimmer (2003). Inclined twins with *exact* coincidence, however, are not known,[8] but *approximate* coincidences (obliquity small but not equal to 0, 'reticular pseudomerohedry'; Friedel, 1926) exist.

Whereas the $\Sigma 3$ twins of rhombohedral and cubic crystals, treated in §§2 to 4, are quite frequent, the tetragonal $\Sigma 5$ twins are relatively rare. There are old indications of a (120)$\Sigma 5$ twin of a cubic garnet (Azruni, 1887; Tschermak & Becke, 1921), but these findings have not been confirmed until now. The first substantial report on this twinning was given by Panina *et al.* (1995), who studied the $\Sigma 5$ microtwinning of synthetic Cr^{4+}- and B^{3+}-doped gehlenite $Ca_2Al(AlSi)O_7$ (point group $\bar{4}2m$) by X-ray diffraction. Later it was shown by the X-ray studies of Bindi *et al.* (2003) and of Gemmi *et al.* (2007) that $\Sigma 5$ twinning occurs in all mixed crystals of the binary melilite solid-solution series [end members gehlenite $Ca_2Al(AlSi)O_7$ and åkermanite $Ca_2MgSi_2O_7$]. It was also shown that this twinning is due to a (120) pseudo-mirror plane of the melilite structure. Tetragonal (120) $\Sigma 5$ twinning was also observed in crystals of $SmS_{1.9}$ (space group *P*4/*n*; Tamazyan *et al.*, 2000), in rare-earth borides (space group *P*4/*ncc*; Oeckler *et al.*, 2002) and in the structure family $X_9Sb_5O_5$ with *X* = Pr, Sm and Dy (space group *P*4/*n*; Nuss & Jansen, 2007). In all these studies the crystal structures were determined by X-ray diffraction of twinned crystals.

5.1. Basis-vector relations

The $\Sigma 5$ twin is based on the twin reflection planes *m*(120) and *m*(310) or the twofold twin axes $2[\bar{2}10]$ and $2[\bar{1}30]$ (parallel to the corresponding twin reflection planes). For the two centrosymmetric groups the reflection planes and the twofold axes represent the same twin law, for the five non-centrosymmetric groups they lead to two different twin laws. For an easier understanding of the twin-related superimposed reflections of the *m*(120) twin, the basis vectors $\mathbf{a}_2$, $\mathbf{b}_2$, $\mathbf{c}_2$ of twin partner 2 are in this section generated from the right-handed basis vectors $\mathbf{a}_1$, $\mathbf{b}_1$, $\mathbf{c}_1$ of the starting partner 1 by the twin reflection *m*(120) itself (Fig. 4), thus forming a left-handed reference system. A treatment by right-handed basis vectors $\mathbf{a}_3$, $\mathbf{b}_3$, $\mathbf{c}_3$, usually applied in structure determinations (*cf.* Tamazyan *et al.*, 2000; Nuss & Jansen, 2007) is presented in Appendix *C*.

The right-handed basis vectors $\mathbf{a}_T$, $\mathbf{b}_T$, $\mathbf{c}_T$ (red in Fig. 4) of the $\Sigma 5$ coincidence lattice are related to the right-handed $\mathbf{a}_1$, $\mathbf{b}_1$, $\mathbf{c}_1$ vectors (green) and left-handed $\mathbf{a}_2$, $\mathbf{b}_2$, $\mathbf{c}_2$ (blue) by

$$\begin{aligned} \mathbf{a}_T &= 2\mathbf{a}_1 - \mathbf{b}_1 &&= 2\mathbf{a}_2 - \mathbf{b}_2 \\ \mathbf{b}_T &= \mathbf{a}_1 + 2\mathbf{b}_1 &&= -\mathbf{a}_2 - 2\mathbf{b}_2 \\ \mathbf{c}_T &= \mathbf{c}_1 = \mathbf{c}_2 \end{aligned}$$

with the supercell parameters $a_T = 5^{1/2}a_1 = 5^{1/2}a_2$, $b_T = 5^{1/2}b_1 = 5^{1/2}b_2$, $c_T = c_1 = c_2$ and $V_T = 5V_1 = 5V_2$.

The reverse transformations are presented by

$$\begin{aligned} \mathbf{a}_1 &= (2\mathbf{a}_T + \mathbf{b}_T)/5, \quad \mathbf{b}_1 = (-\mathbf{a}_T + 2\mathbf{b}_T)/5, \quad \mathbf{c}_1 = \mathbf{c}_T \\ \mathbf{a}_2 &= (2\mathbf{a}_T - \mathbf{b}_T)/5, \quad \mathbf{b}_2 = (-\mathbf{a}_T - 2\mathbf{b}_T)/5, \quad \mathbf{c}_1 = \mathbf{c}_T. \end{aligned}$$

The transformations between the basis vectors $\mathbf{a}_1$, $\mathbf{b}_1$, $\mathbf{c}_1$ (start) and $\mathbf{a}_2$, $\mathbf{b}_2$, $\mathbf{c}_2$ are

$$\begin{aligned} \mathbf{a}_2 &= (3\mathbf{a}_1 - 4\mathbf{b}_1)/5, \quad \mathbf{b}_2 = (-4\mathbf{a}_1 - 3\mathbf{b}_1)/5, \quad \mathbf{c}_2 = \mathbf{c}_1 \\ \mathbf{a}_1 &= (3\mathbf{a}_2 - 4\mathbf{b}_2)/5, \quad \mathbf{b}_1 = (-4\mathbf{a}_2 - 3\mathbf{b}_2)/5, \quad \mathbf{c}_1 = \mathbf{c}_2. \end{aligned}$$

Note that the transformation $\mathbf{a}_1, \mathbf{b}_1, \mathbf{c}_1 \leftrightarrow \mathbf{a}_2, \mathbf{b}_2, \mathbf{c}_2$ is reversible (binary operation). Its determinant is -1, indicating the change of handedness.

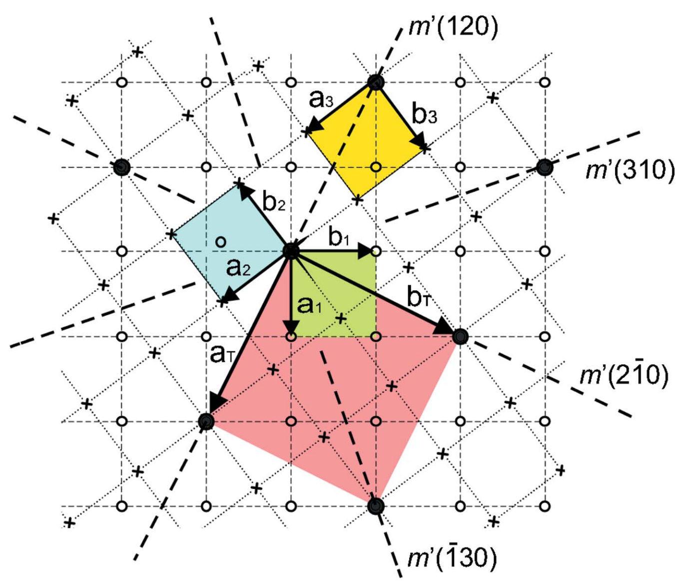

Figure 4
Tetragonal lattices (**a**–**b** planes, common *c* axis pointing upwards) of twin domain I (start domain, lattice points small circles, right-handed green unit cell $\mathbf{a}_1$, $\mathbf{b}_1$, $\mathbf{c}_1$), of the $\Sigma 5$ twin-related domain II (small crosses, left-handed blue unit cell $\mathbf{a}_2$, $\mathbf{b}_2$, $\mathbf{c}_2$) and the $\Sigma 5$ coincidence lattice (large black points, right-handed red unit cell $\mathbf{a}_T$, $\mathbf{b}_T$, $\mathbf{c}_T$). The four alternative twin reflection planes $m'(120)$, $m'(2\bar{1}0)$, $m'(310)$ and $m'(\bar{1}30)$ are indicated by dashed lines. The coordinate axes $\mathbf{a}_2$, $\mathbf{b}_2$, $\mathbf{c}_2$ of domain II (blue) are defined by the reflection plane $m'(120)$. The right-handed yellow unit cell $\mathbf{a}_3$, $\mathbf{b}_3$, $\mathbf{c}_3$ of domain II is obtained from $\mathbf{a}_1$, $\mathbf{b}_1$, $\mathbf{c}_1$ by a clockwise rotation of $\varphi = 2\arctan(1/2) = 53.13°$ around the tetragonal *c* axis (*cf.* Appendix *C*). This cell is commonly used in structure determinations.

[8] Exact lattice coincidence is, in principle, not possible because the coincidence is not enforced by symmetry as it is in the case of 'parallel *c*-axis' twins. It may occur, however, for a certain temperature if the thermal expansion is anisotropic.

The basis-vector relations of the rotation twin $2[2\bar{1}0]$ are easily derived from the equations above: the transformations for the basis vectors $\mathbf{a}_1$, $\mathbf{b}_1$ and $\mathbf{a}_2$, $\mathbf{b}_2$ remain the same, whereas $\mathbf{c}_2$ is inverted: $\mathbf{c}_2 = -\mathbf{c}_1 = -\mathbf{c}_T$, thus forming a right-handed basis.

5.2. Coincidence features of X-ray reflections

The transformations between the Miller indices (HKL) of the (coincidence) supercell and the indices ($h_1k_1l_1$) and ($h_2k_2l_2$) of the twin-related partners 1 (start) and 2 are (*cf.* Fig. 5)

$$H = 2h_1 - k_1 = 2h_2 - k_2$$
$$K = h_1 + 2k_1 = -h_2 - 2k_2$$
$$L = l_1 = l_2$$

$$h_1 = (2H + K)/5, \quad k_1 = (-H + 2K)/5, \quad l_1 = L$$
$$h_2 = (2H - K)/5, \quad k_2 = (-H - 2K)/5, \quad l_2 = L$$

$$h_2 = (3h_1 - 4k_1)/5, \quad k_2 = (-4h_1 - 3k_1)/5, \quad l_2 = l_1$$
$$h_1 = (3h_2 - 4k_2)/5, \quad k_1 = (-4h_2 - 3k_2)/5, \quad l_1 = 1_2.$$

For the $2[2\bar{1}0]$ rotation twin it is $l_2 = -l_1 = -L$.

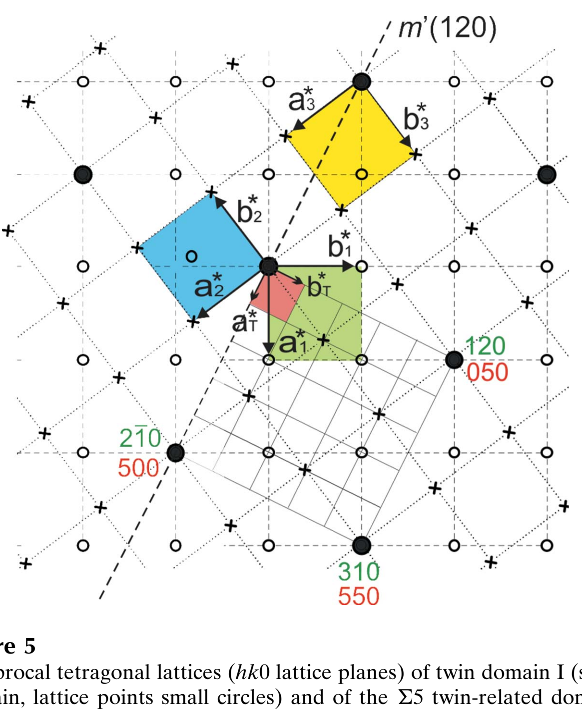

Figure 5
Reciprocal tetragonal lattices ($hk0$ lattice planes) of twin domain I (start domain, lattice points small circles) and of the Σ5 twin-related domain II (small crosses). The reciprocal lattice of the (direct-space) Σ5 coincidence lattice is represented by the grid of small squares. The unit cells, their handedness and their colours correspond to those of the direct lattices in Fig. 4. In the square formed by the four reciprocal coincidence points 000, $2\bar{1}0$, 310, 120 (in terms of $\mathbf{a}_1$*, $\mathbf{b}_1$*) or 000, 500, 550, 050 (in terms of $\mathbf{a}_T$*, $\mathbf{b}_T$*) there are four 'single' points of twin domains I and II each, one 'coincident' point 000 and, with reference to $\mathbf{a}_T$*, $\mathbf{b}_T$*, 16 'extinct' reciprocal points (*cf.* Table 1). These strange 'non-space-group extinctions' are characteristic of the Σ5 twin law.

Most of the transformations $(h_1k_1l_1) \rightarrow (h_2k_2l_2)$ lead to fractional indices in the twin-related domain II, *i.e.* these reflections of the starting domain I are 'single' in the diffraction record. Only those special reflections of domain I, which simultaneously obey the two *coincidence conditions*

$$3h_1 - 4k_1 = 5h_2 = 5N \text{ and } -4h_1 - 3k_1 = 5k_2 = 5M$$
$$(N, M = \text{integers including } 0),$$

lead to integer indices ($h_2k_2l_2$), *i.e.* reflections ($h_1k_1l_1$) and ($h_2k_2l_2$) coincide. They have either equal or different F moduli, representing diffraction cases A, B1 or B2. The two coincidence conditions can be simplified by a mathematical transformation into a single condition:

$$h_1 + 2k_1 = 5P \text{ (with } P \text{ different from } N \text{ and } M).$$

For the re-transformation $(h_2k_2l_2) \rightarrow (h_1k_1l_1)$ the *coincidence condition* is the same:

$$h_2 + 2k_2 = 5P.$$

From the above coincidence conditions it follows that $h_1^2 + k_1^2 = h_2^2 + k_2^2 = 5Q$ (Q integer[9]), *i.e.* they imply that the d values of the twin-related reflections $h_1k_1l_1$ and $h_2k_2l_2$ are equal, a necessary condition for coincidence.[10] For example: twin-related coincident reflections $29l$ and $67l$: $h_1^2 + k_1^2 = h_2^2 + k_2^2 = 85$, $Q = 17$.

The coinciding reflections represent 1/25 of all reflections (*cf.* Table 1). This is demonstrated in Fig. 5: within the cell formed by the four reciprocal coincidence points 000, 120, $2\bar{1}0$, 310 (in terms of $\mathbf{a}_1$*, $\mathbf{b}_1$*) or 000, 500, 550, 050 (in terms of $\mathbf{a}_T$*, $\mathbf{b}_T$*) there are four single points of twin domains I and II each, one coincident point 000 and, with reference to $\mathbf{a}_T$*, $\mathbf{b}_T$*, 16 'extinct' reciprocal points (*cf.* Table 2).

5.3. Group-theoretical considerations, possible Σ5 twins

For the tetragonal holohedry $4/m2/m2m$ as well as the centrosymmetric group $4/m$, the intersection group of the symmetries of the two twin partners is $4/m$. The reduced oriented composite symmetry (twin symmetry) is $4/m2'/m'2'/m'$, with m' and $2'$ representing the following coset of eight alternative twin reflection planes and twin axes (*cf.* Fig. 4):

$m'(120)$, $m'(\bar{2}10)$, $2'[120]$, $2'[\bar{2}10]$ (second position of the point-group symbol);

$m'(310)$, $m'(\bar{1}30)$, $2'[310]$, $2'[\bar{1}30]$ (diagonal reflection planes and axes, third position).

These eight twin elements belong to the same coset and thus represent *one* twin law. For the non-centrosymmetric groups, however, the four twin reflection planes m' and the four twin axes $2'$ represent *different* cosets and thus different twin laws.

A special case is provided by point groups $\bar{4}$ and $\bar{4}2m/\bar{4}m2$ because their twins are reflection as well as rotation twins, *i.e.*

[9] $Q = (k_1 - 2P)^2 + P^2 = (h_1 - P)^2/4 + P^2$ for coincidence condition $h_1 + 2k_1 = 5P$; similar for h_2, k_2 with $h_2 + 2k_2 = 5P$.
[10] The d values of reflections hkl of a tetragonal crystal are given by $1/d^2 = (h^2 + k^2)/a^2 + l^2/c^2$. Since l^2/c^2 is the same for both twin-related reflections, the d values are equal for equal $h^2 + k^2$.

Table 8
Intersection point groups and (oriented) reduced composite groups of the 12 possible tetragonal $\Sigma5$ twins.

The twins in point groups $\bar{4}$ and $\bar{4}2m$, as well as in the centrosymmetric groups $4/m$ and $4/m2/m2/m$, are reflection as well as rotation twins, see text. Note that the symbols of the (oriented) reduced composite groups refer to the tetragonal axes $\mathbf{a}_T$, $\mathbf{b}_T$, $\mathbf{c}_T$ of the coincidence lattice.

Tetragonal point group	Twin intersection group	Twin law	Reduced composite group
4	4	m' $2'$	$4m'm'$ $42'2'$
$\bar{4}$	$\bar{4}$	$m'_{(120)}/2'_{[310]}$ $2'_{[120]}/m'_{(310)}$	$\bar{4}m'2'$ $\bar{4}2'm'$
$4/m$	$4/m$	m', $2'$	$4/m2'/m'2'/m'$
422	4	m' $2'$	$4m'm'$ $42'2'$
$4mm$	4	m' $2'$	$4m'm'$ $42'2'$
$\bar{4}m2$, $\bar{4}2m$	$\bar{4}$	$m'_{(120)}/2'_{[310]}$ $2'_{[120]}/m'_{(310)}$	$\bar{4}m'2'$ $\bar{4}2'm'$
$4/m2/m2/m$	$4/m$	m', $2'$	$4/m2'/m'2'/m'$

their cosets contain two reflection planes and two twofold axes. They are:

(1) $m'(120)$, $m'(\bar{2}10)$, $2'[310]$, $2'[\bar{1}30]$ (reduced composite group $\bar{4}m'2'$) and

(2) $2'[120]$, $2'[\bar{2}10]$, $m'(310)$, $m'(\bar{1}30)$ (reduced composite group $\bar{4}2'm'$).

The intersection and the reduced oriented composite symmetries for the 12 possible tetragonal $\Sigma5$ twins are listed in Table 8.

5.4. Intensity relations of superimposed twin-related reflections

In the following only those reflections of the two twin partners are considered which are both present (*i.e.* not 'single') and superimposed. Again, the sets of symmetry-equivalent reflections *hkl* are geometrically represented by their corresponding face forms {*hkl*}.

Two types of face forms (reflection sets) are distinguished:

(*a*) Face forms {12*l*} and {31*l*} (more generally {*h*.2*h*.*l*} and {3*h*.*h*.*l*} with $h, l = 0, \pm1, \pm2, \ldots$). They include the (di)-tetragonal prisms {*h*.2*h*.0} and the pedion and pinacoid {00*l*}. These forms have special orientations for the $\Sigma5$ twins, because their oriented *eigensymmetries* contain, fully or partly ('splitting' of forms, see below), the eight twin elements $m'(120)$, $m'(310)$ and $2'[120]$, $2'[310]$ *etc*. and thus are, fully or partly, mapped by a twin element upon themselves (diffraction case A) or upon their acentric inverted forms (diffraction case B2, see below).

(*b*) All other face forms {*hkl*}. Their oriented *eigensymmetries* do not contain a twin element, but they may be mapped (fully or partly) upon another non-equivalent face form, leading to diffraction case B1.

These cases are further discussed for the mono-axial groups 4, $\bar{4}$ and $4/m$, and the poly-axial groups 422, $4mm$, $\bar{4}2m$ and $4/m2/m2/m$ separately.

(i) Mono-axial groups 4, $\bar{4}$ and $4/m$ (Table 8):

Type (*a*) face forms:

Reflection twins $m'(120)$ *and* $m'(310)$. All mono-axial forms, tetragonal pyramids and bipyramids {12*l*} and {31*l*}, prisms {120} and {310}, as well as pedion and pinacoid {00*l*}, are mapped upon themselves (Fig. 6). Thus, the twin-related reflections have equal *F* moduli and exhibit diffraction case A.

Special cases are again the tetragonal disphenoids ('tetragonal tetrahedra') {12*l*} and {31*l*} of point group $\bar{4}$, because for this group the twin elements $m'(120)/2'[310]$ and $m'(310)/2'[120]$ represent *different twin laws* (*cf*. their cosets in §5.3) and form simultaneously reflection and rotation twins. For $m'(120)$ and $2'[310]$ twins the disphenoid {12*l*} is mapped upon itself (diffraction case A), whereas the disphenoid {31*l*} is transformed into its inverted ('opposite') form (diffraction case B2). Similarly for twin law $m'(310)/2'[120]$: here the form {31*l*} provides diffraction case A and form {12*l*} diffraction case B2.

Rotation twins $2'[120]$ *and* $2'[310]$. All mono-axial tetragonal bipyramids {12*l*} and {31*l*} and prisms {120} and {310} and the pinacoid {00*l*} are mapped upon themselves and form

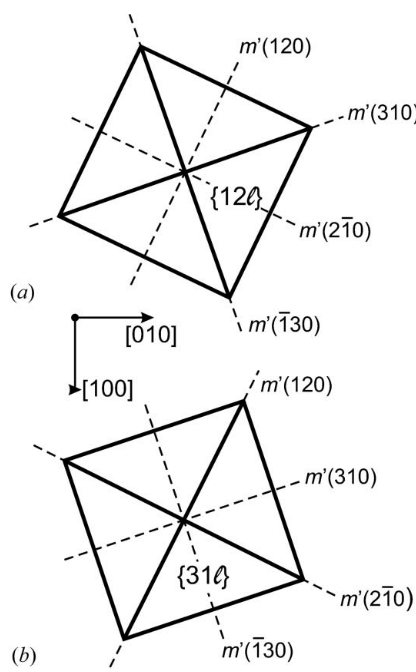

Figure 6
Face forms tetragonal *pyramid* {12*l*} and {31*l*}, projected along the common tetragonal axis, and the coset of the four alternate $\Sigma5$ twin reflection planes m'. These planes belong to the oriented *eigensymmetries* of both forms, which are mapped upon themselves by this twinning. Thus, the corresponding reflection sets {12*l*} and {31*l*} are superimposed with their twin-related sets and have equal *F* moduli (diffraction case A). For the tetragonal *bipyramids*, four additional twofold axes (parallel to the traces of the mirror planes m') belong to their *eigensymmetry* and the twin law. These coincidence and intensity characteristics hold, more generally, for the sets {*h*, 2*h*, *l*}and {3*h*, *h*, *l*} with *h*, *l* any positive or negative integer, including the limiting cases of tetragonal prisms ($l = 0$) and pedion or pinacoid ($h = 0$).

diffraction case A. The tetragonal pyramids and the pedion, however, are mapped upon their opposite forms and thus provide diffraction case B2 (Bijvoet sets). The special case of point group $\bar{4}$ and its face form 'tetragonal disphenoid' is already treated above under 'reflection twins'.

Type (*b*) face forms:

The oriented *eigensymmetries* of all other mono-axial face forms $\{hkl\}$ of type (*b*) (which are the majority) do *not contain* the twin elements $m'(120)$ or $2'[120]$. These forms are either single or mapped upon a non-equivalent form. The *F* moduli of the corresponding reflection sets are different and the reflection intensities depend on the volume ratio of the twin partners (diffraction case B1). Examples are the twin-related reflection sets $\{29l\}/\{67l\}$, $\{17l\}/\{55l\}$ and $\{43l\}/\{05l\}$ with equal $(h^2 + k^2)$ values. This is shown for the set $\{29l\}/\{67l\}$ in Fig. 8.

With regard to the following consideration of poly-axial groups it is emphasized that *all* reflection sets $\{21l\}$, which are related to sets $\{12l\}$ [type (*a*) above, diffraction case A] by reflection through (100) or (110) or by the corresponding twofold rotations, do *not* have a coinciding twin-related counterpart, they are *always* 'single' (*cf.* Fig. 7).

(ii) Poly-axial groups 422, 4*mm*, $\bar{4}2m$ and 4/*m*2/*m*2/*m* (Table 8):

In these groups ditetragonal face forms $\{hkl\}_{\rm ditetr}$ occur. The superposition and intensity relations of the corresponding twin-related reflection sets can be reduced to the mono-axial case above by splitting these forms into two 'mono-axial' subforms $\{hkl\}_{\rm mono}$ (generated by the corresponding mono-axial group) and $\{khl\}_{\rm mono}$, related to $\{hkl\}_{\rm mono}$ by the reflection planes (100) or (110) or the corresponding twofold axes. For example, the face form $\{12l\}_{\rm ditetr}$ is split into the subforms $\{12l\}_{\rm mono}$ and $\{21l\}_{\rm mono}$, which behave as described above in (i): the reflection subset $\{12l\}_{\rm mono}$ [(type (*a*) above] is superimposed upon its twin-related equivalent subset (diffraction cases A or B2), whereas the other subset $\{21l\}_{\rm mono}$ and its twin-related counterpart do not coincide and are each 'single'. This is shown in Fig. 7. It also holds for the special case of the tetragonal scalenohedron $\{12l\}_{\rm ditetr}$ of point group $\bar{4}2m$, which is split into the disphenoids $\{12l\}_{\rm mono}$ [type (*a*), diffraction cases A or B2] and $\{21l\}_{\rm mono}$ ('single').

Similar relations hold for all other (general) ditetragonal face forms of type (*b*) above: each subset $\{hkl\}_{\rm mono}$ is superimposed upon its – now *non-equivalent* – twin-related counterpart (diffraction case B1), whereas subset $\{khl\}_{\rm mono}$ and its twin counterpart do not coincide ('single' reflection sets); this applies also to the (general) tetragonal scalenohedron $\{hkl\}$ of point group $\bar{4}2m$. For example, consider the twin-related face forms (reflection sets) $\{29l\}_{\rm ditetr}$ and $\{67l\}_{\rm ditetr}$: the subsets $\{29l\}_{\rm mono}$ and $\{67l\}_{\rm mono}$ are superimposed (*cf.* Fig. 8*c*), whereas the subsets $\{92l\}_{\rm mono}$ and $\{76l\}_{\rm mono}$ are both 'single' (*cf.* Fig. 8*d*). These *ditetragonal* reflection sets are called here 'partly coincident'. The diffraction cases of twin-related reflection sets for all tetragonal point groups are listed in Table 9.

Finally, the effect of the *I*-lattice centring and of the extinctions in non-symmorphic space groups is considered. It should be noted that, owing to the inclination of the twin elements m' and $2'$ to the secondary symmetry elements of the space group, only the 'coincidence pairs' (doubly coincident reflections, first line in Table 1, large dots in Fig. 5) need to be considered. The 'single reflections' of both domains (lines 2 and 3 in Table 1) exhibit the unmodified space-group extinctions and can be used to determine the space group of the (untwinned) crystal.

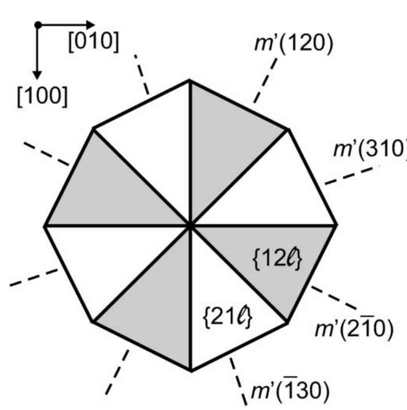

Figure 7
Ditetragonal (bi)-pyramid $\{12l\}_{\rm ditetr}$, a combination of subforms$\{12l\}_{\rm tetr}$ (shaded) and $\{21l\}_{\rm tetr}$ (white). Subset $\{12l\}_{\rm tetr}$ is mapped upon itself by the $\Sigma5$ twin elements (diffraction case A, *cf.* Fig. 6), whereas subset $\{21l\}_{\rm tetr}$ has no twin-related coinciding counterpart and is 'single' ('partial coincidence').

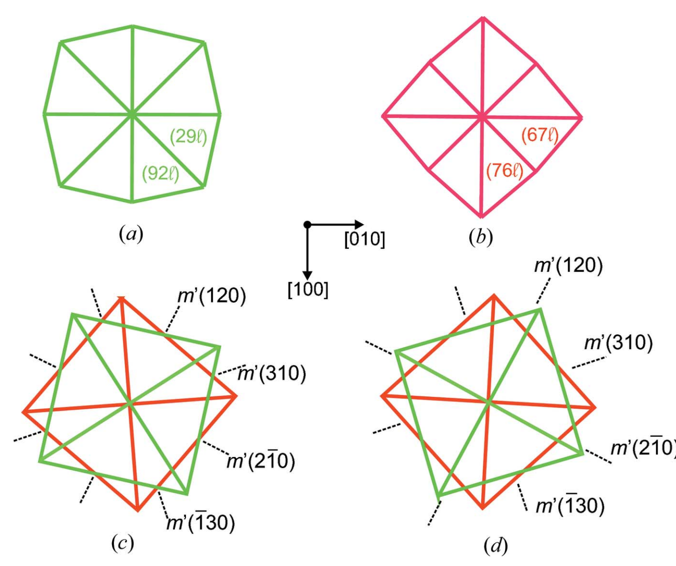

Figure 8
(*a*), (*b*) Non-equivalent ditetragonal (bi)-pyramids $\{29l\}_{\rm ditetr}$ (green) and $\{67l\}_{\rm ditetr}$ (red), both with $h^2 + k^2 = 85$, *i.e.* equal *d* values. (*c*) Mono-tetragonal (bi)-pyramids $\{29l\}$ (green) and $\{67l\}$ (red). The twin elements m' do *not* belong to the *eigensymmetries* of these subforms, but *map them upon each other*. Thus, the corresponding reflection subsets are coincident but have different *F* moduli (diffraction case B1). (*d*) Associated mono-tetragonal (bi)-pyramids $\{92l\}$ (green) and $\{76l\}$ (red). These subforms are *not mapped* upon each other: the corresponding reflection subsets are 'single'. This 'partial coincidence' holds for all general ditetragonal sets $\{2h.9h.l\}$ and $\{6h.7h.l\}$ (except for the pedion/pinacoid, $h = 0$). The same coordinate system is used for all reflections.

Table 9
Twin diffraction cases of coincident twin-related reflection sets $\{hkl\}$ for the 12 tetragonal $\Sigma 5$ twin laws, $m'(120)/(310)$ and $2'[120]/[310]$.

Tetragonal point group	Twin law	Face forms (reflection sets) $\{00l\}$	$\{12l\}$, $\{31l\}$	$\{120\}$, $\{310\}$	All others†
4	m'	A	A	A	'Single' or B1 if coincident
	$2'$	B2	B2	A	
$\bar{4}$	m'	A	A, B2	A	
	$2'$	A	B2, A	A	
$4/m$	m', $2'$	A	A	A	
422	m'	A	A†	A†	'Single' or B1 if (partly) coincident
	2	A	A†	A†	
$4mm$	m'	A	A†	A†	
	$2'$	B2	B2†	A†	
$\bar{4}2m$, $\bar{4}m2$	m'	A	A†, B2†	A†	
	$2'$	A	B2†, A†	A†	
$4/m2/m2/m$	m', $2'$	A	A†	A†	

† Splitting into two subforms: partial coincidence (see text).

(*a*) Coincidence behaviour of $\Sigma 5$ twins with an I lattice. It can be shown that for two coincident twin-related reflection sets $\{h_1k_1l_1\} \leftrightarrow \{h_2k_2l_2\}$ ($l_1 = l_2$), $h_2 + k_2$ is even or odd when $h_1 + k_1$ is even or odd. Thus, the I-reflection condition $h_2 + k_2 + l_1 = 2m$ is obeyed if $h_1 + k_1 + l_2 = 2n$ is fulfilled, *i.e.* the $\Sigma 5$ coincidence lattice is also an I lattice, and a superposition of I-lattice extinct and non-extinct reflections does not occur.

(*b*) Screw axes 4_1, 4_2 and 4_3 have no effect because the fourfold axis is preserved by the twinning, *i.e.* there is no superposition of extinct and non-extinct reflections. The same applies to the c-, a/b- and n-glide planes in I space groups (but not to d-glide planes).

(*c*) In contrast, superposition of extinct and non-extinct reflections occurs in the c-, a/b- and n-glide planes and the $2_1\langle 100\rangle$ and $2_1\langle 110\rangle$ screw axes of P space groups.

6. Σ7 twins of hexagonal and trigonal crystals

These twins and their derivation are very similar to the $\Sigma 5$ twins of tetragonal crystals. The analogies and differences are summarized as follows:

(i) The hexagonal and trigonal 'twins by reticular merohedry with parallel c axes', treated here, do not depend on the hexagonal axial ratio c/a, *i.e.* they can occur in any hexagonal or trigonal crystal (the rhombohedral $\Sigma 3$ twins are treated in §3). This twinning is a two-dimensional phenomenon, *i.e.* the distribution of coincident, single and extinct reflections is the same for all reciprocal layers $hk0$, $hk\pm1$, $hk\pm2$ *etc.* of the twin partners.

(ii) The lowest Σ value for a hexagonal or trigonal 'parallel c-axis twin' is 7. These twins are either reflection twins $m'(12\bar{3}0)$ and their hexagonal equivalents $m'(\bar{3}120)$ and $m'(2\bar{3}10)$, or twofold rotation twins $2'[2\bar{1}0]$ with equivalents $2'[130]$ and $2'[\overline{32}0]$, generating a coincidence lattice of index $h^2 + hk + k^2 = 7$ and $u^2 - uv + v^2 = 7$, respectively. An actual twin of $\Sigma 7$ or higher Σ value ($\Sigma 13$, $\Sigma 19$ *etc.*) is not yet known.

(iii) Twins by reticular merohedry with inclined c axes are also possible but only for special c/a ratios. Theoretical cases have been derived by Grimmer (1989*a*).

(iv) The hexagonal 'crystal family' treated here consists of 12 point groups, seven hexagonal and five trigonal (with four centrosymmetric groups $\bar{3}$, $\bar{3}2/m$, $6/m$, $6/m2/m2/m$), in contrast to only seven tetragonal and five cubic point groups.

6.1. Basis-vector relations

In analogy to §5.1, the hexagonal basis-vector relations for the starting domain I ($\mathbf{a}_1$, $\mathbf{b}_1$, $\mathbf{c}_1$, right-handed), the $\Sigma 7$ coincidence lattice ($\mathbf{a}_T$, $\mathbf{b}_T$, $\mathbf{c}_T$, right-handed) and the reflection twin-related domain II ($\mathbf{a}_2$, $\mathbf{b}_2$, $\mathbf{c}_2$, left-handed, mirror image of $\mathbf{a}_1$, $\mathbf{b}_1$, $\mathbf{c}_1$) are given below (*cf.* Fig. 9):

$$\begin{array}{ll} \mathbf{a}_T = 2\mathbf{a}_1 - \mathbf{b}_1 & = 2\mathbf{a}_2 - \mathbf{b}_2 \\ \mathbf{b}_T = \mathbf{a}_1 + 3\mathbf{b}_1 & = -3\mathbf{a}_2 - 2\mathbf{b}_2 \\ \mathbf{c}_T = \mathbf{c}_1 & = \mathbf{c}_2 \\ \mathrm{Det} = +7 & \mathrm{Det} = -7 \end{array}$$

with the supercell parameters $a_T = b_T = 7^{1/2}a_1 = 7^{1/2}b_1$, $c_T = c_1 = c_2$ and $V_T = 7V_1 = 7V_2$.

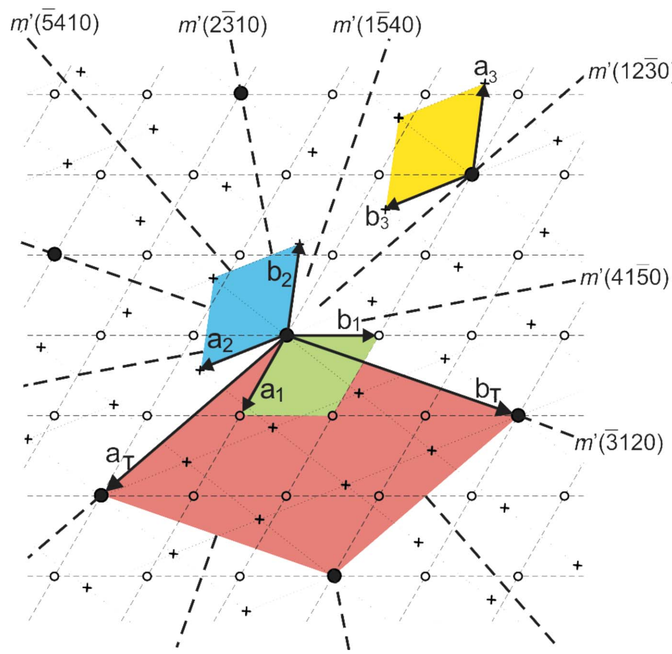

Figure 9
Hexagonal lattices (**a**–**b** planes, common c axis pointing upwards) of twin domain I (start domain, lattice points small circles, right-handed green unit cell $\mathbf{a}_1$, $\mathbf{b}_1$, $\mathbf{c}_1$), of the $\Sigma 7$ twin-related domain II (small crosses, left-handed blue unit cell $\mathbf{a}_2$, $\mathbf{b}_2$, $\mathbf{c}_2$) and of the $\Sigma 7$ coincidence lattice (large black points, right-handed red unit cell $\mathbf{a}_T$, $\mathbf{b}_T$, $\mathbf{c}_T$). The six alternative twin reflection planes $m'(12\bar{3}0)$, $m'(\bar{3}120)$, $m'(2\bar{3}10)$, $m'(\bar{5}410)$, $m'(1\bar{5}40)$ and $m'(41\bar{5}0)$ are indicated by dashed lines. The coordinate axes $\mathbf{a}_2$, $\mathbf{b}_2$, $\mathbf{c}_2$ of domain II (blue) are defined by the reflection plane $m'(12\bar{3}0)$. The right-handed yellow unit cell $\mathbf{a}_3$, $\mathbf{b}_3$, $\mathbf{c}_3$ of domain II is obtained from $\mathbf{a}_1$, $\mathbf{b}_1$, $\mathbf{c}_1$ by a clockwise rotation of $\varphi = 120° + 2\arcsin[(1/2)(3/7)^{1/2}] = 120° + 38.2° = 158.2°$ around the hexagonal axis (*cf.* Appendix *C*). This cell is commonly used in structure determinations.

Reverse transformations:

$$\begin{array}{ll} \mathbf{a}_1 = (3\mathbf{a}_T + \mathbf{b}_T)/7 & \mathbf{a}_2 = (2\mathbf{a}_T - \mathbf{b}_T)/7 \\ \mathbf{b}_1 = (-\mathbf{a}_T + 2\mathbf{b}_T)/7 & \mathbf{b}_2 = (-3\mathbf{a}_T - 2\mathbf{b}_T)/7 \\ \mathbf{c}_1 = \mathbf{c}_T & \mathbf{c}_2 = \mathbf{c}_T \\ \mathrm{Det} = +1/7 & \mathrm{Det} = -1/7. \end{array}$$

Transformations between the basis vectors $\mathbf{a}_1$, $\mathbf{b}_1$, $\mathbf{c}_1$ (start) and $\mathbf{a}_2$, $\mathbf{b}_2$, $\mathbf{c}_2$ (twin-related):

$$\begin{array}{ll} \mathbf{a}_2 = (3\mathbf{a}_1 - 5\mathbf{b}_1)/7 & \mathbf{a}_1 = (3\mathbf{a}_2 - 5\mathbf{b}_2)/7 \\ \mathbf{b}_2 = (-8\mathbf{a}_1 - 3\mathbf{b}_1)/7 & \mathbf{b}_1 = (-8\mathbf{a}_2 - 3\mathbf{b}_2)/7 \\ \mathbf{c}_2 = \mathbf{c}_1 & \mathbf{c}_1 = \mathbf{c}_2 \\ \mathrm{Det} = -1 & \mathrm{Det} = -1. \end{array}$$

The transformations $\mathbf{a}_1$, $\mathbf{b}_1$, $\mathbf{c}_1 \leftrightarrow \mathbf{a}_2$, $\mathbf{b}_2$, $\mathbf{c}_2$ are reversible (binary operations). Their determinants are Det = −1, indicating the change of handedness.

Similar to the tetragonal Σ5 twin, the basis-vector relations of the *rotation* twin $2[2\bar{1}0]$ are easily derived from the equations above: the transformations for the basis vectors $\mathbf{a}_1$, $\mathbf{b}_1$ and $\mathbf{a}_2$, $\mathbf{b}_2$ remain the same, whereas $\mathbf{c}_2$ is inverted: $\mathbf{c}_2 = -\mathbf{c}_1 = -\mathbf{c}_T$, thus forming a right-handed basis.

6.2. Coincidence features of X-ray reflections

The transformations between the Miller indices (HKL) of the (coincidence) supercell and the indices ($h_1k_1l_1$) and ($h_2k_2l_2$) of the reflection twin-related partners 1 (start) and 2 are (*cf.* Fig. 10):

$$\begin{array}{ll} H = 2h_1 - k_1 & = 2h_2 - k_2, \\ K = h_1 + 3k_1 & = -3h_2 - 2k_2 \\ L = l_1 & = l_2 \\ \mathrm{Det} = +7 & \mathrm{Det} = -7 \end{array}$$

$$\begin{array}{ll} h_1 = (3H + K)/7 & h_2 = (2H - K)/7 \\ k_1 = (-H + 2K)/7 & k_2 = (-3H - 2K)/7 \\ l_1 = L & l_2 = L \\ \mathrm{Det} = 1/7 & \mathrm{Det} = -1/7 \end{array}$$

$$\begin{array}{ll} h_2 = (3h_1 - 5k_1)/7 & h_1 = (3h_2 - 5k_2)/7 \\ k_2 = (-8h_1 - 3k_1)/7 & k_1 = (-8h_2 - 3k_2)/7 \\ l_2 = l_1 & l_1 = l_2 \\ \mathrm{Det} = -1 & \mathrm{Det} = -1. \end{array}$$

For the $2[2\bar{1}0]$ *rotation* twin the (h_1, k_1) ↔ (h_2, k_2) transformations are the same, but $l_2 = -l_1 = -L$ and Det = +1.

Most of the transformations ($h_1k_1l_1$) → ($h_2k_2l_2$) (lowest block above) lead to fractional indices in the twin-related domain II, *i.e.* the reflections ($h_1k_1l_1$) of the starting domain I are 'single' in the diffraction record. Only those special reflections, which simultaneously obey the *coincidence conditions*

$$3h_1 - 5k_1 = 7h_2 = 7N \quad \text{and} \quad -8h_1 - 3k_1 = 7k_2 = 7M,$$
$$(N, M \text{ integers including } 0)$$

lead to integer indices ($h_2k_2l_2$), *i.e.* reflections ($h_1k_1l_1$) and ($h_2k_2l_2$) coincide. They have either equal or different F moduli, representing diffraction cases A, B1 or B2. The two coincidence conditions can be simplified by a mathematical transformation into a single condition:

$$2h_1 - k_1 = 7P \ (P = \text{integer, different from } N \text{ and } M).$$

The *coincidence condition* is the same for the re-transformation ($h_2k_2l_2$) → ($h_1k_1l_1$):

$$2h_2 - k_2 = 7P.$$

From these conditions it follows (again by a mathematical transformation) that $h_1^2 + h_1k_1 + k_1^2 = h_2^2 + h_2k_2 + k_2^2 = 7Q$ (Q integer[11]), *i.e.* that the d values of the coincident twin-related reflections $h_1k_1l_1$ and $h_2k_2l_2$ are equal, as expected.[12] For example, consider twin-related reflections $h_1k_1l_1 = 9.\overline{10}.l$ and $h_2k_2l_2 = 11.\bar{6}.l$ ($P = 4$): $h_1^2 + h_1k_1 + k_1^2 = h_2^2 + h_2k_2 + k_2^2 = 91$, $Q = 13$.

The coinciding reflections represent 1/49 of all reflections (*cf.* Table 1). This is demonstrated by Fig. 10: within the cell

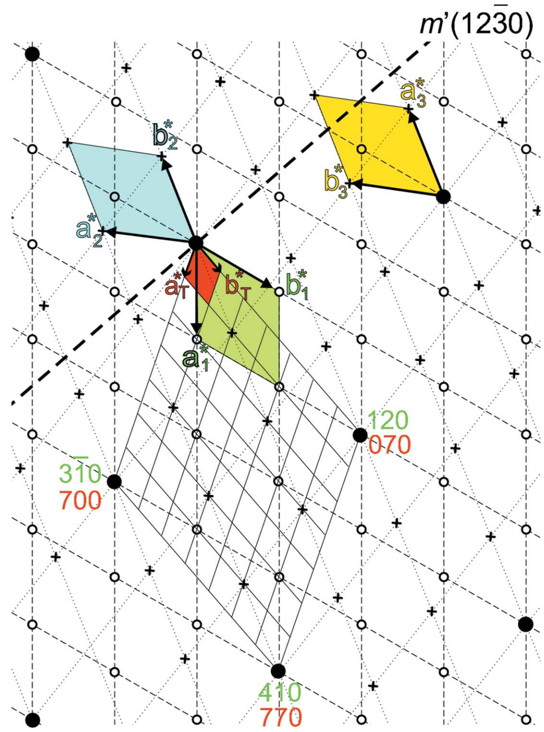

Figure 10
Reciprocal hexagonal lattices ($hk0$ lattice planes) of twin domain I (start domain, lattice points small circles) and of the Σ7 twin-related domain II (small crosses). The reciprocal lattice of the (direct-space) Σ7 coincidence lattice is represented by the grid of small rhombuses. The unit cells, their handedness and their colours correspond to those of the direct lattices in Fig. 9. In the large cell formed by the four reciprocal coincidence points 000, $3\bar{1}0$, 410, 120 (in terms of $\mathbf{a}_1^*$, $\mathbf{b}_1^*$) or 000, 700, 770, 070 (in terms of $\mathbf{a}_T^*$, $\mathbf{b}_T^*$) there are six 'single' points of twin domains I and II each, one 'coincident' point 000 and, with reference to $\mathbf{a}_T^*$, $\mathbf{b}_T^*$, 36 'extinct' reciprocal points (*cf.* Table 1). These strange 'non-space-group extinctions' are characteristic of the Σ7 twin law.

[11] $Q = 7P^2 + h_1(h_1 - 5P) = [7P^2 + k_1(k_1 + 4P)]/4$ for coincidence condition $2h_1 - k_1 = 7P$. The same holds for h_2, k_2 and condition $2h_2 - k_2 = 7P$.

[12] The d values of reflections hkl of a hexagonal crystal are given by $1/d^2 = (h^2 + hk + k^2)/a^2 + l^2/c^2$. Since l^2/c^2 is the same for both twin-related reflections, the d values are equal for equal $h^2 + hk + k^2$.

formed by the four coincident reciprocal-lattice points 000, $3\bar{1}0$, 410, 120 (in terms of $\mathbf{a}_1^*$, $\mathbf{b}_1^*$) or 000, 700, 770, 070 (in terms of $\mathbf{a}_T^*$, $\mathbf{b}_T^*$) there are six single points of twin domains I and II each, one coincident point 000 and, with reference to $\mathbf{a}_T$,* $\mathbf{b}_T$*, 36 'extinct' reciprocal-lattice points.

6.3. Group-theoretical considerations, possible Σ7 twins

For the highest point-group symmetry of the hexagonal crystal family, $6/m2/m2m$ of order 24, the twin intersection group of the two twin partners is $6/m$ (order 12). The 12 operations of the coset (twin law) of the oriented reduced composite symmetry $6/m2'/m'2'/m'$ are partitioned into four subsets of three symmetrically equivalent twin operations each:

1(a) twin reflection planes: $m'(12\bar{3}0)$, $m'(\bar{3}120)$, $m'(2\bar{3}10)$;
1(b) twofold twin axes: $2'[450]$, $2'[\bar{5}\bar{1}0]$, $2'[1\bar{4}0]$;
2(a) twin reflection planes: $m'(\bar{5}410)$, $m'(1\bar{5}40)$, $m'(41\bar{5}0)$;
2(b) twofold twin axes: $2'[2\bar{1}0]$, $2'[130]$, $2'[\bar{3}\bar{2}0]$.

Proper combinations of these four subsets produce the 'cosets of alternative twin elements' for all eight hexagonal and eight trigonal point groups ('structural settings'), as shown in Table 10. All these structural settings are subgroups of index 1 to 8 of the hexagonal holohedral point group $6/m2/m2m$.

6.3.1. Hexagonal point groups. From Table 10 it can be concluded that point groups $6/m$ and $6/m2/m2/m$, both with twin intersection group $6/m$ and reduced composite group $6/m2'/m'2'/m'$, have the full coset consisting of all four subsets with 12 twin operations, whereas all other hexagonal groups with twin intersection groups 6 or $\bar{6}$ have only six twin operations, formed by various combinations of two of the four subsets.

Note that all twins are either pure reflection or rotation twins, except for the centrosymmetric groups $6/m$ and $6/m2/m2m$, the cosets of which contain six reflection and six rotation operations. Similarly, the cosets of point group $\bar{6}$ and the two 'structural settings' $\bar{6}m2$ and $\bar{6}2m$ contain three reflections and three rotations each, *i.e.* the twins of these point groups are reflection as well as rotation twins. In total, there are 14 possible hexagonal Σ7 twins (Table 10).

6.3.2. Trigonal point groups. Each of the five trigonal point groups is a (normal) subgroup of index 2 of one or two hexagonal point groups (symbolized by <):

$3 < 6$ and $\bar{6}$; $\bar{3} < 6/m$; $32 < 622$ and $\bar{6}2m$; $3m < 6mm$ and $\bar{6}m2$; $\bar{3}2/m < 6/m2/m2/m$.

This subgroup degradation is accompanied by a splitting of the three poly-axial groups 32, $3m$ and $\bar{3}2/m$ into two different subgroups: 321/312, $3m1/31m$ and $\bar{3}2/m1/\bar{3}12/m$ ('structural settings').[13] For the mono-axial groups 3 and $\bar{3}$ no splitting into different 'structural settings' occurs.

As a consequence, the cosets of the trigonal point groups contain half as many elements as the cosets of their hexagonal supergroups: two subsets (six elements) each for the centrosymmetric groups/settings $\bar{3}$, $\bar{3}2/m1$ and $\bar{3}12/m$ and one subset (three elements) each for all other trigonal groups/settings, resulting in the unusually large number of 26 possible trigonal Σ7 twins (Table 10). Again, all twins are either reflection or rotation twins, with the exception of the centrosymmetric groups $\bar{3}$, $\bar{3}2/m1$ and $\bar{3}12/m$, which are both reflection and rotation twins.

6.4. Intensity relations of superimposed twin-related reflections

Again, only those reflections of the two twin partners are considered which are *both* present (not 'single') and coincident. Two categories of the corresponding face forms (reflection sets) are distinguished (*cf.* §5.4):

(a) Face forms pyramids $\{12\bar{3}l\}$ and $\{\bar{5}41l\}$ (more generally $\{h.2h.\bar{3}h.l\}$ and $\{\bar{5}h.4h.h.l\}$) (Table 11). They include the (di)-hexagonal and (di)-trigonal prisms (l = 0) and the pedion/pinacoid (h = 0). By the Σ7 twinning these hexagonal forms are (fully or partially) mapped upon themselves (diffraction case A) or upon their opposite forms (diffraction case B2). For the twins of the trigonal point groups, however, besides diffraction cases A and B2, diffraction case B1 also occurs (Table 11).

(b) All other face forms $\{hkil\}$. They are either 'single' or are mapped (fully or partially) upon a non-equivalent form, leading to diffraction case B1.

Again, mono-axial and poly-axial groups are distinguished. In the mono-axial groups coincident twin-related hexagonal/trigonal face forms $\{hkil\}_{\rm hex}/\{hkil\}_{\rm trig}$ are always *fully coincident*, whereas in the poly-axial groups di-hexagonal/di-trigonal forms $\{hkil\}_{\rm dihex}/\{hkil\}_{\rm ditrig}$ are only 'partially coincident', *i.e.* they are split into two mono-hexagonal/mono-trigonal subforms $\{hkil\}_{\rm hex}/\{hkil\}_{\rm trig}$ and $\{khil\}_{\rm hex}/\{khil\}_{\rm trig}$, one of which is 'coincident' with its twin-related partner (always diffraction case B1) and the other is 'single'. In the majority of general $hkil$ cases *both* mono-axial sets are 'single'. All these cases can be illustrated in the same way as for the Σ5 twins (Figs. 6–8). The diffraction cases of twin-related reflection sets for all hexagonal and trigonal point groups are listed in Table 11.

Rhombohedral (R) centring. The effect of the rhombohedral centring of a hexagonal lattice on the Σ7 twinning is somewhat complicated: depending on the Σ7 twin element two different cases can occur. As for the Σ5 twins in §5.4, only the coincidence lattice $\mathbf{a}_T$, $\mathbf{b}_T$, $\mathbf{c}_T$ (red in Fig. 9) and the 'doubly non-extinct' coincident reflections (first line in Table 1, large dots in Fig. 10) need to be considered. The 'single' reflections of both domains (lines 2 and 3 in Table 1, small crosses and circles in Fig. 10) and their extinctions belong to the untwinned domains and can be used to determine the space group of the (untwinned) crystal and the twin law.

It is assumed that the starting domain I (green cell $\mathbf{a}_1$, $\mathbf{b}_1$, $\mathbf{c}_1$ in Fig. 9) exhibits 'obverse' centring; hexagonal axes are used throughout.

(i) If the Σ7 twin element is one of the three symmetrically equivalent reflection planes $(12\bar{3}0)$, $(\bar{3}120)$, $(2\bar{3}10)$ with

[13] The reduced composite symmetries are the same for $3m1$ and $31m$ *etc.*, because the twin elements $m'(12\bar{3}0)$ *etc.* are the same for both groups. For details of 'structural settings', see Klapper & Hahn (2010), Appendix *A*.

Table 10
Twin intersection point groups, twin laws (cosets) and reduced (oriented) composite groups for the eight hexagonal and eight trigonal 'structural settings', resulting in 14 hexagonal and 26 trigonal $\Sigma 7$ twin laws.

The number of twin laws for each point group (structural setting) is given in column 1 in parentheses. The twins are either pure reflection or pure rotation twins. In point groups $\overline{6}$ and $\overline{6}2m/\overline{6}m2$, as well as in the four centrosymmetric point groups, however, they are reflection as well as rotation twins, see text. The symbols of the reduced (oriented) composite groups refer to the hexagonal axes $\mathbf{a}_T$, $\mathbf{b}_T$, $\mathbf{c}_T$ of the coincidence lattice. Note that all (untwinned) point groups and structural settings with the same twin intersection group have the same twin laws (cosets) and the same reduced composite groups (*i.e.* groups 6, 622 and $6mm$; $\overline{6}$, $\overline{6}m2$ and $\overline{6}2m$; $6/m$ and $6/m2/m2/m$; 3, 321, 312, $3m1$ and $31m$; $\overline{3}$, $\overline{3}2/m1$ and $\overline{3}12/m$), but nevertheless represent different twin cases. For details of the twin laws (cosets) see §6.3.

Point group, structural settings (No. of twin laws)	Twin intersection group	Twin law (cosets)	Reduced oriented composite group
Hexagonal point groups			
6 (2)	6	m': 1(a) + 2(a)	$6m'm'$
		$2'$: 1(b) + 2(b)	$62'2'$
$\overline{6}$ (2)	$\overline{6}$	$m' + 2'$: 1(a) + 2(b)	$\overline{6}m'2'$
		$2' + m'$: 1(b) + 2(a)	$\overline{6}2'm'$
$6/m$ (1)	$6/m$	$2'/m' + 2'/m'$: 1(a) + 1(b) + 2(a) + 2(a)	$6/m2'/m'2'/m'$
622 (2)	6	m': 1(a) + 2(a)	$6m'm'$
		$2'$: 1(b) + 2(b)	$62'2'$
$6mm$ (2)	6	m': 1(a) + 2(a)	$6m'm'$
		$2'$: 1(b) + 2(b)	$62'2'$
$\overline{6}m2$, $\overline{6}2m$ (2 + 2)	$\overline{6}$	$m' + 2'$: 1(a) + 2(b)	$\overline{6}m'2'$
		$2' + m'$: 1(b) + 2(a)	$\overline{6}2'm'$
$6/m2/m2/m$ (1)	$6/m$	$2'/m' + 2'/m'$: 1(a) + 1(b) + 2(a) + 2(a)	$6/m2'/m'2'/m'$
Trigonal point groups			
3 (4)	3	m': 1(a)	$3m'1$
		m': 2(a)	$31m'$
		$2'$: 1(b)	$32'1$
		$2'$: 2(b)	$312'$
$\overline{3}$ (2)	$\overline{3}$	$2'/m'1$: 1(a) + 1(b)	$\overline{3}2'/m'1$
		$12'/m'$: 2(a) + 2(b)	$\overline{3}12'/m'$
321, 312 (4 + 4)	3	m': 1(a)	$3m'1$
		m': 2(a)	$31m'$
		$2'$: 1(b)	$32'1$
		$2'$: 2(b)	$312'$
$3m1$, $31m$ (4 + 4)	3	m': 1(a)	$3m'1$
		m': 2(a)	$31m'$
		$2'$: 1(b)	$32'1$
		$2'$: 2(b)	$312'$
$\overline{3}2/m1$, $\overline{3}12/m$ (2 + 2)	$\overline{3}$	$2'/m'1$: 1(a) + 1(b)	$\overline{3}2'/m'1$
		$12'/m'$: 2(a) + 2(b)	$\overline{3}12'/m'$

$h^2 + hk + k^2 = 7$ *or* one of the three perpendicular equivalent twofold axes [450], $[\overline{5}\overline{1}0]$, $[\overline{1}40]$ with $u^2 - uv + v^2 = 21$, the direct-space coincidence lattice is *not* R-centred but primitive (red cell $\mathbf{a}_T$, $\mathbf{b}_T$, $\mathbf{c}_T$ in Fig. 9), because no rhombohedral centring points of the two twin domains coincide. Hence, the reciprocal coincidence lattice has the same cell (large dots) as in Fig. 10: $00l$, $70l$, $77l$, $07l$ with l = 0 and 3, without any 'doubly extinct' points.

(ii) If the $\Sigma 7$ twin elements are rotated around [001] by 30° (or 90°) compared to those in (i), *i.e.* if the twin element is one of the three equivalent reflection planes $(41\overline{5}0)$, $(\overline{5}410)$, $(1\overline{5}40)$ with $h^2 + hk + k^2 = 21$, *or* one of the three perpendicular equivalent twofold axes [320], $[\overline{2}10]$, [130] with $u^2 - uv + v^2 = 7$, the direct-space coincidence lattice is R-centred (obverse), with (doubly coincident) centring points in 2/3, 1/3, 1/3 and 1/3, 2/3, 2/3. This triple direct cell leads to a triply diluted reciprocal coincidence cell [compared to case (i) above] formed by the points $00l$, $21.0.l$, $21.21.l$, $0.21.l$ with l = 0 and 3, which contains the following 'doubly non-extinct' reflections:

$$l = 0\text{: } 000, 770, 14.14.0,$$
$$l = 1\text{: } 701, 0.14.1, 14.7.1,$$
$$l = 2\text{: } 072, 14.0.2, 7.14.2.$$

Space-group extinctions. The space-group extinctions of non-symmorphic space groups have rather simple effects for $\Sigma 7$ twins, because in *trigonal* and *hexagonal* crystals only screw axes along [001] and two types of c-glide planes occur: $h0\overline{h}l, l = 2n$ (example $P3c1$) and $hh\overline{2h}l, l = 2n$ (example $P31c$). Both conditions exist in $P6cc$. In *rhombohedral* crystals only $h0\overline{h}l, l = 2n$ occurs in $R3c$ and $R\overline{3}c$. The effect of these symmetry elements upon the $\Sigma 7$ twins can be summarized as follows:

(i) All extinctions of $\{000l\}$ reflection sets, due to threefold and sixfold screw axes, coincide for both twin domains, because their c axes are parallel.

(ii) Because the $\Sigma 7$ twin planes are inclined to the secondary and tertiary c-glide planes, only the 'coincident' reflections (first line in Table 1, large dots in Fig. 10) need to be considered.

(iii) *Hexagonal* space groups with c-glide planes: For $l = 2n + 1$ extinct reflections fall on non-extinct ones, whereas for $l = 2n$ the coincidence pairs are non-extinct. There are no 'doubly extinct' reflections.

(iv) *Rhombohedral* space groups with c-glide planes: For $h0\overline{h}l, l = 2n + 1$, extinct ($c$-glide) reflections fall either on non-extinct or on extinct (R-lattice) reflections, depending upon the value of l (= $6n \pm 3$ or = $6n \pm 1$) and the type of twin element (see above). For l = $2n$ the coincidences in $R3c$ and $R\overline{3}c$ are unchanged compared to $R3m$ and $R\overline{3}m$. However, now $l = 6n$ is the period along **c** of the reciprocal coincidence lattice (reflections $000l$ occur only for $l = 6n$), in contrast to $l = 3n$ for the symmorphic rhombohedral space groups.

Table 11
Twin diffraction cases of coincident twin-related reflection sets (face forms) $\{hkil\}$ for the 14 hexagonal and 26 trigonal $\Sigma 7$ twin laws $m'(12\bar{3}0)$, $2'[450]$, $m'(\bar{5}410)$ and $2'[2\bar{1}0]$.

Diffraction cases of di-hexagonal/di-trigonal face forms (reflection sets) are marked with *. They are split into the 'mono' subforms $\{12\bar{3}l\}$ and $\{\bar{5}41l\}$ which are 'coincident', and the associated subforms $\{21\bar{3}l\}$ and $\{4\bar{5}1l\}$ which are 'single' ('partial coincidence', see text). Diffraction cases separated by a comma (*e.g.* A, B2) refer to the different $\{hkil\}$ forms given at the top of columns 4 and 5; a slash (*e.g.* A/A) separates entries for the two structural settings listed in column 1.

		Face forms (reflection sets)			
Point group	Twin law	$\{000l\}$	$\{12\bar{3}l\}$, $\{\bar{5}41l\}$	$\{12\bar{3}0\}$, $\{\bar{5}410\}$	All others†
Hexagonal point groups					
6	m'	A	A	A	Single or B1 if coincident
	$2'$	B2	B2	A	
$\bar{6}$	$m' + 2'$	A	B2, A	B2, A	
	$2' + m'$	A	A, B2	A, B2	
$6/m$	$2'/m' + 2'/m'$	A	A	A	
622	m'	A	A*	A*	Single or B1 if (partly) coincident*
	2	A	B2*	A*	
$6mm$	m'	A	A*	A*	
	$2'$	B2	B2*	A*	
$\bar{6}m2/\bar{6}2m$	$m' + 2'$	A/A	B2*, A*/A*, B2*	B2*, A*/A*, B2*	
	$2' + m'$	A/A	A*, B2*/B2*, A*	A*, B2*/B2*, A*	
$6/m2/m2/m$	$2'/m' + 2'/m'$	A	A*	A*	
Trigonal point groups					
3	m'	A	B1, A	B2, A	Single or B1 if coincident
	m'	A	A, B1	A, B2	
	$2'$	B2	B1, B2	A, B2	
	$2'$	B2	B2, B1	B2, A	
$\bar{3}$	$2'/m'1$	A	B1, A	A/A	
	$12'/m'$	A	A, B1	A/A	
321/312	m'	A/A	B1*, A*/A*, B1*	B2*, A*/A*, B2*	Single or B1 if (partly) coincident*
	m'	A/A	A*, B1*/B1*, A*	A*, B2*/B2*, A*	
	$2'$	A/A	B1*, B2*/B2*, B1*	B2*, A*/A*, B2*	
	$2'$	A/A	B2*, B1*/B1*, B2*	A*, B1*/B1*, A*	
$3m1/31m$	m'	A/A	B1*, A*/A*, B1*	B2*, A*/A*, B2*	
	m'	A/A	A*, B1*/B1*, A*	A*, B2*/B2*, A*	
	$2'$	B2/B2	B1*, B2*/B2*, B1*	A*, B2*/B2*, A*	
	$2'$	B2/B2	B2*, B1*/B1*, B2*	B2*, A*/A*, B2*	
$\bar{3}2/m1/\bar{3}12/m$	$2'/m'1$	A/A	B1*, A*/A*, B1*	A*/A*	
	$12'/m'$	A/A	A*, B1*/B1*, A*	A*/A*	

† Splitting into two subforms: partial coincidence (see text).

The twin diffraction cases for rhombohedral crystals are the same as for the trigonal crystals in Table 11, except that the extinctions due to the *R*-centring and, if present, due to the $h0\bar{h}l$ *c*-glide have to be taken into account additionally.

7. Conclusion

The present paper completes our treatment of *twinning by* (*reticular*) *merohedry* which was started with the $\Sigma 1$ twins (*complete* lattice coincidence, Klapper & Hahn, 2010) and is continued here with $\Sigma > 1$ twins (*partial* lattice coincidence). Always twins with the lowest possible Σ value for a given crystal system are treated: $\Sigma 3$ twins of rhombohedral and cubic, $\Sigma 5$ twins of tetragonal, and $\Sigma 7$ twins of hexagonal and trigonal crystals. Based on these treatments, the approach can be easily extended to coincidence lattices of higher Σ values.

In the twins treated here the main symmetry axes (threefold, fourfold, sixfold) of all twin domains are always *parallel*. This has the important consequence that the (exact) coincidences of reflection sets ('diffraction cases' A, B1, B2) are independent of the axial ratio *c*/*a* or the rhombohedral angle α of the crystal, in contrast to the twinning by reticular merohedry with *inclined* axes, where lattice coincidences occur only for special axial ratios (*cf*. Grimmer, 1989*a*,*b*, 2003).

The diffraction records of the $\Sigma > 1$ twins with parallel main axes contain 'single' reflections of twin domains I and II each, 'coincident' reflections of both domains and, if referred to the

Σn coincidence cell, doubly 'extinct' reflections. For a given Σ value the ratio of single reflections to coincident reflections is $(\Sigma - 1)$:1 for each of the two domain states [or $2(\Sigma - 1)$:1 for both states], *i.e.* 2:1 for $\Sigma3$, 4:1 for $\Sigma5$ and 6:1 for $\Sigma7$ twins (*cf*. Table 1). Thus, in structure determinations of crystals twinned with high Σ values it may be sufficient to measure only the 'single' reflections of one domain (advisably the one with larger volume) and perform the refinements without the coincident reflections and the volume ratios of the twin partners. This has been shown for a $\Sigma3$ obverse/reverse twin by Wilkens & Müller-Buschbaum (1992) and for a $\Sigma5$ twin by Oeckler *et al.* (2002). The latter compared the results of the structure determinations of a single (untwinned) and a $\Sigma5$ twinned crystal (volume ratio about 50:50), whereby the latter was refined with both the complete diffraction data of the twinned crystal and the data of each of the two domains alone. The inclusion of all reflections yielded only slightly better results than using the data from only one domain. The parameters of the single and the twinned crystal, however, differ somewhat more than their e.s.d.'s indicate. Thus it is expected that in some cases, particularly for twins with $\Sigma \geq 7$, the structure determination and refinement with the diffraction data of the larger domain alone is sufficient. Of course, the nature of the twinning must be recognized beforehand, *e.g.* by unusual 'non-space-group absences' in the diffraction record of the twin (*cf*. §2.1 and Table 2). A real case of a twin with $\Sigma \geq 7$, however, is not known.

A final remark concerns the twins by reticular merohedry with inclined axes. There is no face form (reflection set) that contains a twin element in its *eigensymmetry*. Thus, all coincident reflections are symmetrically non-equivalent and provide B1 diffraction cases. Exceptions are those special (single) faces that are parallel or normal to the twin mirror plane or the twofold twin axis. They are diffraction case A.

Table 12
Merohedral $\Sigma3$ and $\Sigma1$ twin laws of rhombohedral (R) crystals (described in hexagonal axes, top line, and in rhombohedral/cubic axes, bottom line).

(1) *Coset* of subgroup $\bar{3}2/m$ (rhombohedral holohedry, order 12) in supergroup $6/m2/m2/m$ (hexagonal holohedry, order 24), partitioned into four subsets of three alternative twin operations each forming merohedral $\Sigma3$ twins of rhombohedral crystals.

1(*a*)	Sixfold twin rotations	$6^1[001]$ $6^1[111]$	$6^3 = 2[001]$ $6^3 = 2[111]$	$6^5[001]$ $6^5[111]$
1(*b*)	Sixfold twin rotoinversions	$\bar{6}^1[001]$ $\bar{6}^1[111]$	$\bar{6}^3[001] = m(0001)$ $\bar{6}^3[111] = m(111)$	$\bar{6}^5[001]$ $\bar{6}^5[111]$
1(*c*)	Twofold twin rotations	$2[210]$ $2[2\bar{1}\bar{1}]$	$2[\bar{1}10]$ $2[\bar{1}2\bar{1}]$	$2[\bar{1}\bar{2}0]$ $2[\bar{1}\bar{1}2]$
1(*d*)	Twin reflections	$m(10\bar{1}0)$ $m(2\bar{1}\bar{1})$	$m(\bar{1}100)$ $m(\bar{1}2\bar{1})$	$m(0\bar{1}10)$ $m(\bar{1}\bar{1}2)$

(2) *Eigensymmetry* elements of the rhombohedral holohedry $\bar{3}2/m$ (order 12), forming merohedral $\Sigma1$ twins of rhombohedral crystals.

2(*a*)	Threefold rotations	$3^0[001] = 1$ $3^0[111] = 1$	$3^1[001]$ $3^1[111]$	$3^2[001]$ $3^2[111]$
2(*b*)	Threefold rotoinversions	$\bar{3}^1[001]$ $\bar{3}^1[111]$	$\bar{3}^3[001] = \bar{1}$ $\bar{3}^3[111] = \bar{1}$	$\bar{3}^5[001]$ $\bar{3}^5[111]$
2(*c*)	Twofold rotations	$2[100]$ $2[1\bar{1}0]$	$2[010]$ $2[01\bar{1}]$	$2[\bar{1}\bar{1}0]$ $2[\bar{1}01]$
2(*d*)	Reflections	$m(2\bar{1}\bar{1}0)$ $m(1\bar{1}0)$	$m(\bar{1}2\bar{1}0)$ $m(01\bar{1})$	$m(\bar{1}\bar{1}20)$ $m(\bar{1}01)$

Table 13
The 11 $\Sigma3$ and 11 $\Sigma1$ twin laws of the five rhombohedral point groups.

Note that in column 6 the first twin law of each rhombohedral point group (first line, printed in bold) is the *identity* (untwinned crystal). The $\Sigma1$ twins (column 5) are treated in detail in Klapper & Hahn (2010), Table 9.

Point group	Index [n] in $6/m2/m2/m$ (order 24)	Twin composite group and twin law: $\Sigma3$ twins	Twin law	$\Sigma1$ twins	Twin law
3 (order 3)	8	6 $\bar{6}$ 312 $31m$	1(*a*) 1(*b*) 1(*c*) 1(*d*)	3 $\bar{3}$ 321 $3m1$	**2(*a*)** 2(*b*) 2(*c*) 2(*d*)
$\bar{3}$ (order 6)	4	$6/m$ $\bar{3}12/m$	1(*a*) + 1(*b*) 1(*c*) + 1(*d*)	$\bar{3}$ $\bar{3}2/m1$	**2(*a*) + 2(*b*)** 2(*c*) + 2(*d*)
32 (order 6)	4	622 $\bar{6}2m$	1(*a*) + 1(*c*) 1(*b*) + 1(*d*)	321 $\bar{3}2/m1$	**2(*a*) + 2(*c*)** 2(*b*) + 2(*d*)
$3m$ (order 6)	4	$6mm$ $\bar{6}m2$	1(*a*) + 1(*d*) 1(*b*) + 1(*c*)	$3m1$ $\bar{3}2/m1$	**2(*a*) + 2(*d*)** 2(*b*) + 2(*c*)
$\bar{3}2/m$ (order 12)	2	$6/m2/m2/m$	1(*a*) + 1(*b*) + 1(*c*) + 1(*d*)	$\bar{3}2/m1$	**2(*a*) + 2(*b*)** **+ 2(*c*) + 2(*d*)**

APPENDIX *A*
Overview of merohedral $\Sigma1$ and $\Sigma3$ twins of rhombohedral crystals

In Appendix *A* of the previous paper (Klapper & Hahn, 2010, p. 339) the index n of the point group of the 'untwinned crystal' in its holohedral point group was established as the 'order parameter' for the $\Sigma1$ merohedral twins. In particular, for the hexagonal crystal family the maximal value n = 8 represents the 'distance' of the 'hexagonal' point group 3 from the hexagonal holohedry $6/m2/m2/m$ and n = 4 the 'distance' of the 'rhombohedral' point group 3 from the rhombohedral holohedry $\bar{3}2/m$. The relevant $\Sigma 1$ twin laws are listed in Appendix *D*, Tables 9(*c*) and 9(*d*), of Klapper & Hahn (2010).

The results of the present paper permit the extension of the index *n* to both $\Sigma 3$ *and* $\Sigma 1$ twins of rhombohedral crystals: the number of $\Sigma 1$ plus $\Sigma 3$ merohedral twin laws is again n = 2, 4 and 8, even though the distance between point group 3 and its rhombohedral holohedry is only 4. Table 12 lists the four subsets 1(*a*)–1(*d*) for the $\Sigma 3$ twins and the four subsets 2(*a*)–2(*d*) for the $\Sigma 1$ twins, whereas Table 13 gives the 11 combinations of the subsets in the various twin composite groups. Each rhombohedral point group has $n/2$ (= 1, 2 or 4) $\Sigma 3$ and $n/2$ $\Sigma 1$ twin laws. Hence, in all cases *n* twin laws exist, in particular n = 8 different twin laws for point group 3. This way the index 8 appears again as the 'order parameter' for the entire hexagonal crystal family, based both on the rhombohedral and the hexagonal lattice.

The following features are noteworthy:

(i) Among the $\Sigma 1$ twins the 'untwinned' crystal must be taken as the first twin law, just as in any symmetry group the identity 1 is the first symmetry operation. In Tables 9(*c*) and 9(*d*) of Klapper & Hahn (2010) the 'identity twin law' is omitted, *i.e.* only $(n - 1)$ $\Sigma 1$ twin laws are listed.

(ii) Tables 12 and 13 show that for the five point groups 3, $\bar{3}$, 32, 3*m* and $\bar{3}2/m$ the two well known 'obverse/reverse' twin laws 2[001] and *m*(0001), 1(*a*) and 1(*b*) (hexagonal axes), exist. There exist, however, two further independent $\Sigma 3$ twin laws, represented by 2[210] and $m(10\bar{1}0)$, 1(*c*) and 1(*d*). These two $\Sigma 3$ twin laws have not found particular attention in the past. Three experimental cases, however, are reported:

(*a*) In the structure determination of a $\Sigma 3$ twin of $KAu(CN)_2$ (space group $R\bar{3}$) the twin law 2[210] = $m(10\bar{1}0)$, case 1(*c*) and 1(*d*) of Table 13, has been postulated (Rosenzweig & Cromer, 1959).

(*b*) In the 'Example 2' (point group 3), described by Herbst-Irmer & Sheldrick (2002), the following twin laws are mentioned: $\Sigma 3$ twofold twin axis '$\mathbf{a} - \mathbf{b}$', *i.e.* $2[1\bar{1}0]$ = 2[210] [case 1(*c*) in Table 13] and $\Sigma 1$ twofold twin axis '$\mathbf{a} + \mathbf{b}$', *i.e.* 2[110] = 2[100] [case 2(*c*), hexagonal axes]; in addition a possible $\Sigma 1$ inversion twinning is included.

(*c*) In the structure determination of $KAu_xAg_{(1-x)}(CN)_2$ (space group $R\bar{3}$) the $\Sigma 3$ twin law 2[210] = $m(10\bar{1}0)$ has been identified (Hettiarachchi *et al.*, 2007).

(iii) The occurrence of n ($\Sigma 1$ + $\Sigma 3$) twin laws in the five rhombohedral point groups can also be understood as follows: of the *n* possible twin laws, the $n/2$ $\Sigma 1$ cases are represented by twin elements that are symmetry elements of the *rhombohedral holohedry* $\bar{3}2/m$, but not of the point group of the (untwinned) crystal, whereas the $n/2$ $\Sigma 3$ twin laws are formed by twin elements that are symmetry elements of the *hexagonal holohedry* $6/m2/m2/m$, but not of the *rhombohedral holohedry* $\bar{3}2/m$. This shows once more the unique role played by the hexagonal crystal family among the six three-dimensional crystal families (seven crystal systems).

APPENDIX *B*
Splitting of cubic into rhombohedral face forms

The splitting of the various (general and special) face forms $\{hkl\}_{\rm cub}$ of the cubic holohedry $4/m\bar{3}2/m$ into the (general and special) subface forms $\{hkl\}_{\rm rh}$ of its subgroup $\bar{3}2/m$ of index [4] (rhombohedral holohedry), briefly outlined in §4.1, is treated here in more detail. The threefold axis of the subgroup $\bar{3}2/m$ is one of the four threefold axes $\langle 111\rangle$ of the cubic group, here [111] is chosen (which is later the spinel twin axis), and the rhombohedral coordinate axes are the cubic coordinate axes (rhombohedral angle α = 90°).[14]

The crucial parameter for finding the rhombohedral subface forms $\{hkl\}_{\rm rh}$ of the cubic form $\{hkl\}_{\rm cub}$ is $n = h + k + l$. The meaning of *n* becomes apparent by considering the transformation of the rhombohedral indices $\{hkl\}_{\rm rh}$ into hexagonal indices $\{hkil\}_{\rm hex}$ (*cf.* Arnold, 2002):

Obverse setting	Reverse setting
$h_{\rm hex} = h_{\rm rh} - k_{\rm rh}$	$h_{\rm hex} = -h_{\rm rh} + k_{\rm rh}$
$k_{\rm hex} = k_{\rm rh} - l_{\rm rh}$	$k_{\rm hex} = -k_{\rm rh} + l_{\rm rh}$
$i_{\rm hex} = -h_{\rm rh} + l_{\rm rh}$	$i_{\rm hex} = h_{\rm rh} - l_{\rm rh}$
$l_{\rm hex} = h_{\rm rh} + k_{\rm rh} + l_{\rm rh}$	$l_{\rm hex} = h_{\rm rh} + k_{\rm rh} + l_{\rm rh}$.

This shows that $n = h_{\rm rh} + k_{\rm rh} + l_{\rm rh}$ is the hexagonal Bravais–Miller index $l_{\rm hex}$ of the faces $\{hkl\}_{\rm rh}$ with respect to the threefold symmetry axis. Since *all* faces of a rhombohedral form have the *same* Miller index $\pm l_{\rm hex}$, the faces of $\{hkl\}_{\rm cub}$ with equal values of *n* constitute a rhombohedral subform, *i.e.* the different subforms can be distinguished by their different values of $n = h + k + l$. In the rhombohedral subgroups with a polar axis (3 and 3*m*), *n* is either positive or negative for all faces of a form, whereas in the groups with a non-polar axis ($\bar{3}$, 32, $\bar{3}2/m$) one half of the faces of a form has positive, the other half negative $l_{\rm hex} = n$. In the following this simple rule is applied to the general and special forms of the cubic holohedry $4/m\bar{3}2/m$ with subgroup $\bar{3}2/m$ along $[111]_{\rm cub}$.[15]

General face form $\{hkl\}_{cub}$ *of* $4/m\bar{3}2/m$ *(48 faces)*:

The general form $\{hkl\}_{\rm cub}$ of $4/m\bar{3}2/m$ (all indices different and not zero) has the multiplicity 48 (*cf.* Hahn & Klapper, 2002, p. 790), whereas the general form $\{hkl\}_{\rm rh}$ of subgroup $\bar{3}2/m$ has the multiplicity 12. Thus the form $\{hkl\}_{\rm cub}$ must split into four different general subforms $\{hkl\}_{\rm rh}$:[16]

(*a*) $\{hkl\}_{\rm rh}$ with $h + k + l = \pm n_1$
(*b*) $\{\bar{h}\bar{k}l\}_{\rm rh}$ with $-h - k + l = \pm n_2$
(*c*) $\{\bar{h}k\bar{l}\}_{\rm rh}$ with $-h + k - l = \pm n_3$
(*d*) $\{h\bar{k}\bar{l}\}_{\rm rh}$ with $h - k - l = \pm n_4$.

Since the values of n_1, n_2, n_3, n_4 are different, these subforms are also different. They correspond to the identity and to the twofold axes [001], [010] and [100] common to the five cubic

[14] Note that there are four conjugate subgroups $\bar{3}2/m$ of $4/m\bar{3}2/m$ of index [4]. Each of these has a single $\bar{3}$ axis along one of the four body-diagonal $\bar{3}$ axes of the cubic supergroup (*cf.* Müller, 2004, p. 708).
[15] If the subgroup is chosen along one of the other body diagonals $[\bar{1}11]$, $[1\bar{1}1]$ or $[11\bar{1}]$, the types of splitting, given below, remain the same, but the Miller indices of the subforms would change.
[16] They represent the four conjugate subgroups $\bar{3}2/m$ of $4/m\bar{3}2/m$.

supergroups. In the rhombohedral holohedry $\overline{3}2/m$ there are three different types of *general* face forms of multiplicity 12: the '*ditrigonal scalenohedron*' $\{hkl\}_{\rm rh}$, the *limiting general* form '*hexagonal dipyramid*' with the special index combination $\{hk(2k-h)\}_{\rm rh}$, *i.e.* $n = h + k + l = \pm 3k$, and the *limiting general* form '*dihexagonal prism*' with the special index combination $\{hk(\overline{h+k})\}_{\rm rh}$, *i.e.* $n = h + k + l = 0$ (*cf.* Hahn & Klapper, 2002, p. 782 and Fig. 3 of the present paper).

Depending on the values of h, k, l, the following four combinations of subforms may occur:

(*a*) all four subforms are ditrigonal scalenohedra; for example, $\{236\}_{\rm cub}$;

(*b*) three ditrigonal scalenohedra and one hexagonal dipyramid: one of the subforms has the index combination $\{hk(2k-h)\}$ with $n = \pm 3k$; for example, $\{214\}_{\rm cub}$, subform $\{2\overline{1}\overline{4}\}_{\rm rh}$;

(*c*) three ditrigonal scalenohedra and one dihexagonal prism: one of the subforms has the index combination $\{hk(\overline{h+k})\}$ with $n = h + k + l = 0$; for example, $\{347\}_{\rm cub}$, subform $\{34\overline{7}\}_{\rm rh}$;

(*d*) two ditrigonal scalenohedra, one hexagonal bipyramid and one dihexagonal prism: there is one index combination $\{hk(2k-h)\}$ and one with $h + k + l = 0$; for example, $\{123\}_{\rm cub}$, subforms $\{123\}_{\rm rh}$ and $\{12\overline{3}\}_{\rm rh}$ (*cf.* §4.1 and Fig. 3). Note that the general form $\{123\}_{\rm cub}$ and its higher orders $h\{123\}_{\rm cub}$ *are the only ones* that split into *three* different subforms.

Special face forms of $4/m\overline{3}2/m$:

Form {hhl}$_{cub}$ *(24 faces)*. Both types of cubic face forms, trapezohedron ($|h| < |l|$) and trisoctahedron ($|h| > |l|$), *always* split into *three* rhombohedral subforms: $\{hhl\}_{\rm rh}$ (rhombohedron, six faces), $\{hh\overline{l}\}_{\rm rh}$ (rhombohedron, six faces) and $\{\overline{h}hl\}_{\rm rh} = \{h\overline{h}l\}_{\rm rh}$ (ditrigonal scalenohedron, 12 faces). For the special case $l = 2h_{\rm cub}$ the rhombohedron $\{hh\overline{l}\}_{\rm rh}$ degenerates into the hexagonal prism $\{hh\overline{2h}\}_{\rm rh}$; similarly for $l = -2h_{\rm cub}$ in $\{hhl\}_{\rm rh}$.

Form {0kl}$_{cub}$ *(24 faces)*. This form, tetrahexahedron, *always* splits into two different ditrigonal scalenohedra $\{0kl\}_{\rm rh}$ and $\{0\overline{k}l\}_{\rm rh}$ (both 12 faces). For the special case $l = 2k_{\rm cub}$ the subform $\{0k2k\}_{\rm rh}$ is a hexagonal dipyramid (12 faces); the other one, $\{0\overline{k}2k\}_{\rm rh}$, remains a ditrigonal scalenohedron; similarly for $l = -2k_{\rm cub}$.

Form {0kk}$_{cub}$ *(12 faces)*. The rhomb-dodecahedron splits into the two subforms $\{0kk\}_{\rm rh}$ (rhombohedron, six faces) and $\{0k\overline{k}\}_{\rm rh}$ (hexagonal prism, six faces).

Form {hhh}$_{cub}$ *(eight faces)*. The octahedron splits into the subforms $\{hhh\}$ (pinacoid, two faces) and $\{hh\overline{h}\}$ (60° rhombohedron, six faces).

Form {h00}$_{cub}$ *(six faces)*. The cube is a 90° rhombohedron $\{h00\}_{\rm rh}$ (six faces) and does not split.

In the four merohedral cubic groups an additional splitting may occur as a result of the lower symmetry. For example, in the two non-centrosymmetric groups with polar threefold axes, $\overline{4}3m$ and 23, the cube $\{h00\}_{\rm cub}$ is split into two 'opposite' trigonal 90° pyramids $\{h00\}_{\rm rh}$ and $\{\overline{h}00\}_{\rm rh}$.

Special face form {0kk} in the five cubic point groups:

As a further illustration the splitting of the cubic form rhomb-dodecahedron $\{0kk\}_{\rm cub}$ (12 faces) in the five cubic groups is considered. This centrosymmetric form, common to all cubic groups, exhibits a rich variety of splitting into rhombohedral subforms. There are two main rhombohedral subforms in the *centrosymmetric* groups: $\{0k\overline{k}\}$ ($n = 0$, hexagonal prisms) and $\{0kk\}$ (rhombohedra). In the *non-centrosymmetric* groups these are further subdivided into two 'opposite' trigonal prisms and two 'opposite' trigonal 120° pyramids.[17] The twin-related reflections of the sets $\{0k\overline{k}\}$ (prisms) are mapped upon themselves or their antipodes and are *always coincident*. The reflections of the sets $\{0kk\}$, however, are transformed into *absent* reflections $1/3k\{114\}$ (*cf.* index transformations in §3.3). Only the third-order reflections $3N\{0kk\}$ (N integer) coincide with twin-related $Nk\{114\}$ (diffraction case B1), the others are 'single'.

The splitting of the rhomb-dodecahedron $\{0kk\}_{\rm cub}$ into subforms with their specific diffraction cases for the five rhombohedral subgroups is presented in Table 14. Note that the two opposite trigonal prisms $\{0k\overline{k}\}_{\rm rh}$ and $\{0\overline{k}k\}_{\rm rh}$ of intersection groups 3 and 32 are transformed into each other by the twin elements 2[111] and $2[2\overline{1}\overline{1}]$ and thus are formally Bijvoet sets (diffraction case B2). These two sets, not equivalent in the rhombohedral groups, are equivalent in their cubic supergroups and have equal F moduli. Thus, they represent in effect diffraction case A. This particular case is here denoted with $\underline{\rm A}$ (underlined). This fact is due to the centrosymmetric *eigensymmetry* of the form $\{0kk\}_{\rm cub}$ (rhomb-dodecahedron) also in the non-centrosymmetric cubic groups.

Summary of all cubic→rhombohedral split forms and their $\Sigma 3$ *twin diffraction cases*

Table 15 provides a complete list of the rhombohedral subforms of all general, limiting and special cubic face forms of the five cubic point groups, including their diffraction cases for all spinel $\Sigma 3$ twin laws. Details of the list are explained in the following remarks.

Each entry in lines 1–10 contains up to four rhombohedral face forms with in general different values of $n = h + k + l$, consisting of the starting form given in column 1 and the three further forms generated from the first by the twofold axes along $[100]_{\rm cub}$, $[010]_{\rm cub}$ and $[001]_{\rm cub}$ of the cubic supergroup. Owing to the rhombohedral angle $\alpha = 90°$, some or all of these twofold cubic axes may be *eigensymmetry* axes of the (rhombohedral) form generated by them. This means that two of the four forms, or even all four forms, are identical, displaying different but symmetrically equivalent Miller indices. Examples are given in remarks to lines 5, 7, 9 and 10 below.

Line 2: the cubic symbol $\{hk(2k-h)\}_{\rm cub}$ in column 2 stands for the four rhombohedral subforms $\{hk(2k-h)\}_{\rm rh}$ ($n = 3k$), $\{\overline{h}\overline{k}(2k-h)\}_{\rm rh}$ ($n = k - 2h$), $\{\overline{h}k(\overline{2k-h})\}_{\rm rh}$ ($n = -k$) and $\{h\overline{k}(\overline{2k-h})\}_{\rm rh}$ ($n = 2h - 3k$). The first form with $n = 3k$ (pyramids and rhombohedron, *e.g.* {345} with $n = 12$) represents coincident twin-related reflection sets (diffraction cases A, B1, B2), the other three forms represent reflection sets with diffraction cases 'S + B1'.

[17] It is emphasized that the term 'opposite' (*i.e.* related by an inversion) refers here only to the morphology of the two split forms.

Table 14
Splitting of the cubic rhomb-dodecahedron $\{0kk\}_{cub}$ into its rhombohedral subforms in the five cubic point groups and their diffraction cases for the four $\Sigma3$ twin laws.

The symbol $\underline{A}$ indicates diffraction case A due to the symmetry equivalence of all faces of $\{0kk\}_{cub}$ in the cubic group, but it is formally diffraction case B2 in the rhombohedral subgroup. Thus, all trigonal prisms $\{0k\bar{k}\}$ are diffraction case $\underline{A}$ for the twofold twin axes 2[111] and $2[2\bar{1}\bar{1}]$, but diffraction case A for the twin mirror planes $m(111)$ and $m(2\bar{1}\bar{1})$, whereas the rhombohedra and trigonal pyramids are always diffraction case S + B1. In column 5 'S' refers to 'single' reflections for $k \neq 3N$ and 'B1' to coincident reflections for $k = 3N$.

Cubic point group	Rhombohedral [111] subgroup	Rhombohedral split forms (reflection sets)	Multiplicity	Diffraction cases for the twin laws† 2[111], $m(111)$, $2[2\bar{1}\bar{1}]$, $m(2\bar{1}\bar{1})$
23	3	2 opposite trigonal pyramids $\{0kk\}$, $\{0\bar{k}\bar{k}\}$	(3 + 3)	All S + B1
		2 opposite trigonal prisms $\{0k\bar{k}\}$, $\{0\bar{k}k\}$	(3 + 3)	$\underline{A}$, A, $\underline{A}$, A
$2/m\bar{3}$	$\bar{3}$	1 109.47° rhombohedron $\{0kk\}$‡	(6)	All S + B1
		1 hexagonal prism $\{0k\bar{k}\}$	(6)	All A
432	32	1 109.47° rhombohedron $\{0kk\}$‡	(6)	All S + B1
		2 opposite trigonal prisms $\{0k\bar{k}\}$, $\{0\bar{k}k\}$	(3 + 3)	$\underline{A}$, A, $\underline{A}$, A
$\bar{4}3m$	$3m$	2 opposite trigonal pyramids $\{0kk\}$, $\{0\bar{k}\bar{k}\}$	(3 + 3)	All S + B1
		1 hexagonal prism $\{0k\bar{k}\}$	(6)	All A
$4/m\bar{3}2/m$	$\bar{3}2/m$	1 109.47° rhombohedron $\{0kk\}$‡	(6)	All S + B1
		1 hexagonal prism $\{0k\bar{k}\}$	(6)	All A

† The twin laws and their combinations in this column are explained in detail in Appendix *A* and Table 12. ‡ 109.47° = tetrahedral angle = angle between two opposite body diagonals of the cube (= $180° - 2\arctan 2^{-1/2}$).

Line 3: the cubic symbol $\{hk(h+k)\}_{cub}$ in column 2 stands for the four rhombohedral subforms $\{hk(h+k)\}_{rh}$ $(n = 2h + 2k)$, $\{\overline{hk}(h+k)\}_{rh}$ $(n = 0)$, $\{\bar{h}k(\overline{h+k})\}_{rh}$ $(n = -2h)$ and $\{h\bar{k}(\overline{h+k})\}_{rh}$ $(n = -2k)$. The form with $n = 0$ (prisms, *e.g.* $\{\overline{23}5\}$) represents coincident reflection sets (diffraction cases A, B1, B2), the other three forms represent reflection sets with diffraction cases 'S + B1'.

Line 5: the cubic form $\{hh2h\}_{cub}$ splits into the rhombohedral subforms $\{hh2h\}_{rh}$ $(n = 4h)$, $\{\overline{hh}2h\}$ $(n = 0$, prisms), $\{\bar{h}h\overline{2h}\}_{rh}$ $(n = -2h)$ and $\{h\bar{h}\overline{2h}\}_{rh}$ $(n = -2h)$. In the rhombohedral point groups $\bar{3}2/m$ (column 3) and $3m$ (column 4) the latter two sets with equal $n = -2h$ merge into one form, whereas they are different forms in the other three groups (columns 5–7).

Line 7: the cubic face form $\{0k2k\}_{cub}$ is a special case of form $\{0kl\}_{cub}$ in line 6. Its rhombohedral subforms are $\{0k2k)\}_{rh}$ $(n = 3k)$, $\{0\overline{k2k}\}_{rh}$ $(n = -3k)$, $\{0k\overline{2k}\}_{rh}$ $(n = -k)$ and $\{0\bar{k}2k\}_{rh}$ $(n = k)$. There occur two types of combinations of these subforms: in the two centrosymmetric rhombohedral groups $\bar{3}2/m$ and $\bar{3}$ (columns 3 and 6) the two subforms with $n = 3k$ and $n = -3k$, as well as the two subforms with $n = -k$ and $n = k$, are the same, because of centrosymmetry. They form two centrosymmetric face forms, one with diffraction case A, one with diffraction case S + B1. In the non-centrosymmetric groups $3m$, 32 and 3 (columns 4, 5 and 7) the cubic form $\{0k2k\}$ splits into four non-centrosymmetric, but pairwise opposite subforms, one pair with $n = \pm 3k$ exhibits diffraction cases A, $\underline{A}$ and B1, the other pair with $n = \pm k$ provides S + B1.

Line 8: the cubic form $\{0kk\}_{cub}$ is the centrosymmetric rhomb-dodecahedron in all cubic point groups. Its splitting into rhombohedral subforms and their twin diffraction cases are treated in detail above in this Appendix and in Table 14.

Line 9: the cubic form octahedron $\{hhh\}_{cub}$ with rhombohedral split forms $\{hhh\}_{rh}$ $(n = 3h)$, $\{\overline{hh}h\}_{rh}$ $(n = -h)$, $\{\bar{h}h\bar{h}\}_{rh}$ $(n = -h)$, $\{h\overline{hh}\}_{rh}$ $(n = -h)$. The first form $\{hhh\}_{rh}$ represents the pedion or the pinacoid, whereas the following three index triples, all with $n = -h$, represent the same trigonal 60° pyramid (groups $3m$ and 3, columns 4 and 7) or 60° rhombohedron (groups $\bar{3}2/m$, 32 and $\bar{3}$, columns 3, 5, 6).

Line 10: the cube $\{h00\}_{cub}$ with formal rhombohedral split forms $\{h00\}_{rh}$ $(n = h)$, $\{\bar{h}00\}_{rh}$ $(n = -h)$, $\{\bar{h}00\}_{rh}$ $(n = -h)$, $\{h00\}_{rh}$ $(n = h)$. In the three rhombohedral point groups with a *non-polar* threefold axis $\bar{3}2/m$, 32 and $\bar{3}$ $(n = \pm h$, columns 3, 5 and 6) all four index triples represent the same 90° rhombohedron (cube), because the three cubic twofold axes quoted above belong to the *eigensymmetry* of the 90° rhombohedron. In the two *polar* rhombohedral groups $3m$ and 3 (columns 4 and 7) only the two index triples with the same sign of h represent the same form, resulting in the two split forms 'opposite trigonal 90° pyramids'. The splitting results from the loss of the inversion centre of the 90° rhombohedron in the polar groups. For all reflection sets $\{h00\}$ only twin diffraction case 'S + B1' occurs.

APPENDIX *C*

Right-handed coordinate systems of Σ5 and Σ7 reflection twins

C1. Tetragonal Σ5 reflection twins $m'(120)$ and $m'(310)$ with both twin partners based on right-handed coordinate systems

In §5.1 the basis-vector relations are given for the case that the coordinate systems of the two Σ5 twin partners are of opposite handedness, *i.e.* basis vectors and twin domains exhibit the same enantiomorphism. Following international convention, however, both twin partners and their coincidence lattice are usually described in right-handed coordinate systems, even if the twin partners are enantiomorphic. For this

Table 15
Splitting of the general and special cubic face forms into their rhombohedral subforms for all five cubic point groups, and twin diffraction cases of the corresponding reflection sets.

Multiplicities of forms are given in parentheses. The forms printed in bold face provide diffraction cases 'S + B1' for all twin laws, whereby reflections with $n = h + k + l = 3N$ are 'coincident' (B1) and those with $n = h + k + l \neq 3N$ are 'single' (S). The forms printed in normal font represent coincident reflection sets (no 'S' cases) due to the special values $n = 3k$ (special pyramids and rhombohedra) or $n = 0$ (prisms) given in column 2. Their diffraction cases for the up to four different twin laws 2[111], $m(111)$, $2[2\bar{1}\bar{1}]$, $m(2\bar{1}\bar{1})$ and their combinations (one for $\bar{3}2/m$, two for $3m$, 32 and $\bar{3}$, four for 3, *cf.* Appendix *A* and Table 13) are also given ('opp'. means 'opposite', *i.e.* related by an inversion). The symbol $\underline{\text{A}}$ indicates a rhombohedral B2 diffraction case which is A due to the cubic crystal symmetry. For details, see text.

Line	Cubic face form	Splitting of cubic forms into rhombohedral subforms with threefold axis along $[111]_{\text{cub}}$		
		$4/m\bar{3}2/m \rightarrow \bar{3}2/m$	$\bar{4}3m \rightarrow 3m$	$432 \rightarrow 32$
1	$\{hkl\}$	(48): 4 **ditrigonal scalenohedra** (4 × 12)	(24): 4 **ditrigonal pyramids** (4 × 6)	(24): 4 **trigonal trapezohedra** (4 × 6)
2	$\{hk(2k-h)\}$ $n = 3k$	(48): 3 **ditrigonal scalenohedra** (3 × 12) 1 hexagonal bipyramid (12) A	(24): 3 **ditrigonal pyramids** (3 × 6) 1 hexagonal pyramid (6) A/B2	(24): 3 **trigonal trapezohedra** (3 × 6) 1 trigonal bipyramid (6) B2/A
3	$\{hk(h+k\}$ $n = 0$	(48): 3 **ditrigonal scalenohedra** (3 × 12) 1 dihexagonal prism (12) A	(24): 3 **ditrigonal pyramids** (3 × 6) 1 ditrigonal prism (6) B2/A	(24): 3 **trigonal trapezohedra** (3 × 6) 1 ditrigonal prism (6) B2/A
4	$\{hhl\}$	(24): 1 **ditrigonal scalenohedron** (12) 2 **rhombohedra** (2 × 6)	(12): 1 **ditrigonal pyramid** (6) 2 **trigonal pyramids** (2 × 3)	(24): 2 **opp. trigonal trapezohedra** (2 × 6) 2 **rhombohedra** (2 × 6)
5	$\{hh2h\}$ $n = 0$	(24): 1 **ditrigonal scalenohedron** (12) 1 **rhombohedron** (6) 1 hexagonal prism (6) A	(12): 1 **ditrigonal pyramid** (6) 1 **trigonal pyramid** (3) 1 trigonal prism (3) B2/A	(24): 2 **opp. trigonal trapezohedra** (2 × 6) 1 **rhombohedron** (1 × 6) 1 hexagonal prism (1 × 6) A/A
6	$\{0kl\}$	(24): 2 **ditrigonal scalenohedra** (2 × 12)	(24): 4 **ditrigonal pyramids** (4 × 6) (pairwise opp.)	(24): 4 **trigonal trapezohedra** (4 × 6) (pairwise opp.)
7	$\{0k2k\}$ $n = 3k$	(24): 1 **ditrigonal scalenohedron** (12) 1 hexagonal bipyramid (12) A	(24): 2 opp. **ditrigonal pyramids** (2 × 6) 2 opp. hexagonal pyramids (2 × 6) A/$\underline{\text{A}}$	(24): 2 **opp. trigonal trapezohedra** (2 × 6) 2 opp. trigonal bipyramids (2 × 6) $\underline{\text{A}}$/A
8	$\{0kk\}$ $n = 0$	(12): 1 **109.47° rhombohedron** (6) 1 hexagonal prism (6) A	(12): 2 **opp. trigonal 109.47° pyramids** (2 × 3) 1 hexagonal prism (6) A/A	(12): 1 **109.47° rhombohedron** (6) 2 opp. trigonal prisms (2 × 3) $\underline{\text{A}}$/A
9	$\{hhh\}$ $n = 3h$	(8): 1 **60° rhombohedron** (6) 1 pinacoid (2) A	(4): 1 **trigonal 60° pyramid** (3) 1 pedion (1) A/B2	(8): 1 **60° rhombohedron** (6) 1 pinacoid (2) A/A
10	$\{h00\}$	(6): 1 **90° rhombohedron** (6) (cube)	(6): 2 **opp. trigonal 90° pyramids** (2 × 3) $\{h00\}$, $\{\bar{h}00\}$	(6): 1 **90° rhombohedron** (6) (cube)

Line	Cubic face form	Splitting of cubic forms into rhombohedral subforms with threefold axis along $[111]_{\text{cub}}$	
		$2/m\bar{3} \rightarrow \bar{3}$	$23 \rightarrow 3$
1	$\{hkl\}$	(24): 4 **rhombohedra** (4 × 6)	(12): 4 **trigonal pyramids** (4 × 3)
2	$\{hk(2k-h)\}$ $n = 3k$	(24): 3 **rhombohedra** (3 × 6) 1 rhombohedron (6) B1/A	(12): 3 **trigonal pyramids** (3 × 3) 1 trigonal pyramid (3) B1/B1/B2/A
3	$\{hk(h+k\}$ $n = 0$	(24): 3 **rhombohedra** (3 × 6) 1 hexagonal prism (6) A/B1	(12): 3 **trigonal pyramids** (3 × 3) 1 trigonal prism (3) B2/A/B1/B1
4	$\{hhl\}$	(24): 4 **rhombohedra** (4 × 6)	(12): 4 **trigonal pyramids** (4 × 3)
5	$\{hh2h\}$ $n = 0$	(24): 3 **rhombohedra** (3 × 6) 1 hexagonal prism (1 × 6) A/A	(12): 3 **trigonal pyramids** (3 × 3) 1 trigonal prism (3) B2/A/A/B2
6	$\{0kl\}$	(12): 2 **rhombohedra** (2 × 6)	(12): 4 **trigonal pyramids** (4 × 3) (pairwise opp.)
7	$\{0k2k\}$ $n = 3k$	(12): 1 **rhombohedron** (6) 1 rhombohedron (6) B1/A	(12): 2 **opp. trigonal pyramids** (2 × 3) 2 opp. trigonal pyramids (2 × 3) B1/B1/$\underline{\text{A}}$/A
8	$\{0kk\}$ $n = 0$	(12): 1 **109.47° rhombohedron** (6) 1 hexagonal prism (6) A/A	(12): 2 **opp. trigonal 109.47° pyramids** (2 × 3) 2 opp. trigonal prisms (2 × 3) $\underline{\text{A}}$/A/$\underline{\text{A}}$/A
9	$\{hhh\}$ $n = 3h$	(8): 1 **60° rhombohedron** (6) 1 pinacoid (2) A/A	(4): 1 **trigonal 60° pyramid** (3) 1 pedion (1) A/B2/B2/A
10	$\{h00\}$	(6): 1 **90° rhombohedron** (6) (cube)	(6): 2 **opp. trigonal 90° pyramids** (2 × 3) $\{h00\}$, $\{\bar{h}00\}$

reason, the transformation equations between the two right-handed partners $\mathbf{a}_1$, $\mathbf{b}_1$, $\mathbf{c}_1$ (green in Fig. 4) and $\mathbf{a}_3$, $\mathbf{b}_3$, $\mathbf{c}_3$ (yellow) and the right-handed coincidence lattice $\mathbf{a}_T$, $\mathbf{b}_T$, $\mathbf{c}_T$ (red) are given below. Lattice $\mathbf{a}_3$, $\mathbf{b}_3$, $\mathbf{c}_3$ is generated by a clockwise rotation of $\mathbf{a}_1, \mathbf{b}_1, \mathbf{c}_1$ by 53.13° (= 2 arctan 1/2) around the tetragonal c axis.

Coincidence lattice:

$$\begin{array}{ll} \mathbf{a}_T = 2\mathbf{a}_1 - \mathbf{b}_1 & = 2\mathbf{a}_3 + \mathbf{b}_3 \\ \mathbf{b}_T = \mathbf{a}_1 + 2\mathbf{b}_1 & = -\mathbf{a}_3 + 2\mathbf{b}_3 \\ \mathbf{c}_T = \mathbf{c}_1 & = \mathbf{c}_3 \\ \mathrm{Det} = +5 & \mathrm{Det} = +5 \end{array}$$

with the supercell parameters $a_T = 5^{1/2}a_1 = 5^{1/2}a_2$, $b_T = 5^{1/2}b_1 = 5^{1/2}b_2$, $c_T = c_1 = c_3$, $V_T = 5V_1 = 5V_3$.

Reverse transformations:

$$\begin{array}{ll} \mathbf{a}_1 = (2\mathbf{a}_T + \mathbf{b}_T)/5 & \mathbf{a}_3 = (2\mathbf{a}_T - \mathbf{b}_T)/5 \\ \mathbf{b}_1 = (-\mathbf{a}_T + 2\mathbf{b}_T)/5 & \mathbf{b}_3 = (\mathbf{a}_T + 2\mathbf{b}_T)/5 \\ \mathbf{c}_1 = \mathbf{c}_T & \mathbf{c}_3 = \mathbf{c}_T \\ \mathrm{Det} = +5 & \mathrm{Det} = +5. \end{array}$$

Transformations between the basis vectors $\mathbf{a}_1$, $\mathbf{b}_1$, $\mathbf{c}_1$ (start, green in Fig. 4) and $\mathbf{a}_3$, $\mathbf{b}_3$, $\mathbf{c}_3$ (yellow):

$$\begin{array}{ll} \mathbf{a}_1 = (3\mathbf{a}_3 + 4\mathbf{b}_3)/5 & \mathbf{a}_3 = (3\mathbf{a}_1 - 4\mathbf{b}_1)/5 \\ \mathbf{b}_1 = (-4\mathbf{a}_3 + 3\mathbf{b}_3)/5 & \mathbf{b}_3 = (4\mathbf{a}_1 + 3\mathbf{b}_1)/5 \\ \mathbf{c}_1 = \mathbf{c}_3 & \mathbf{c}_3 = \mathbf{c}_1 \\ \mathrm{Det} = +1 & \mathrm{Det} = +1. \end{array}$$

Note that the second power of the latter transformations $(\mathbf{a}_1, \mathbf{b}_1, \mathbf{c}_1) \leftrightarrow (\mathbf{a}_3, \mathbf{b}_3, \mathbf{c}_3)$ is not the identity transformation, but rather a rotation of 2 × 53.13° = 106.26°, in contrast to the corresponding ('binary') transformations $(\mathbf{a}_1, \mathbf{b}_1) \leftrightarrow (\mathbf{a}_2, \mathbf{b}_2)$ in §5.1.

The equations for transformations of the Miller indices hkl do not need to be given since they are the same as those of the basis vectors, as can be seen by comparing §§5.1 and 5.2.

C2. Hexagonal Σ7 reflection twins $m'(12\bar{3}0)$ and $m'(\bar{5}410)$ with both twin partners based on right-handed coordinate systems

In analogy to §C1 above, the relations between the three right-handed coordinate systems $\mathbf{a}_1$, $\mathbf{b}_1$, $\mathbf{c}_1$ (green in Fig. 9), $\mathbf{a}_T$, $\mathbf{b}_T$, $\mathbf{c}_T$ (red) and $\mathbf{a}_3$, $\mathbf{b}_3$, $\mathbf{c}_3$ (yellow) are given below, the latter generated by a clockwise rotation of $\mathbf{a}_1$, $\mathbf{b}_1$, $\mathbf{c}_1$ by 158.2° {= 120° + 2 arcsin $[1/2\,(3/7)^{1/2}]$} around the hexagonal axis (*cf.* Fig. 9).

Coincidence lattice:

$$\begin{array}{ll} \mathbf{a}_T = 2\mathbf{a}_1 - \mathbf{b}_1 & = -\mathbf{a}_3 + 2\mathbf{b}_3 \\ \mathbf{b}_T = \mathbf{a}_1 + 3\mathbf{b}_1 & = -2\mathbf{a}_3 - 3\mathbf{b}_3 \\ \mathbf{c}_T = \mathbf{c}_1 & = \mathbf{c}_3 \\ \mathrm{Det} = +7 & \mathrm{Det} = +7 \end{array}$$

with supercell parameters $a_T = 7^{1/2}a_1 = 7^{1/2}a_2$, $b_T = 7^{1/2}b_1 = 7^{1/2}b_2$, $c_T = c_1 = c_3$, $V_T = 7V_1 = 7V_3$.

Reverse transformations:

$$\begin{array}{ll} \mathbf{a}_1 = (3\mathbf{a}_T + \mathbf{b}_T)/7 & \mathbf{a}_3 = (-3\mathbf{a}_T - 2\mathbf{b}_T)/7 \\ \mathbf{b}_1 = (-\mathbf{a}_T + 2\mathbf{b}_T)/7 & \mathbf{b}_3 = (2\mathbf{a}_T - \mathbf{b}_T)/7 \\ \mathbf{c}_1 = \mathbf{c}_T & \mathbf{c}_3 = \mathbf{c}_T \\ \mathrm{Det} = +1/7 & \mathrm{Det} = +1/7. \end{array}$$

Transformations between $\mathbf{a}_1$, $\mathbf{b}_1$, $\mathbf{c}_1$ (start, green in Fig. 9) and $\mathbf{a}_3$, $\mathbf{b}_3$, $\mathbf{c}_3$ (yellow):

$$\begin{array}{ll} \mathbf{a}_1 = (-5\mathbf{a}_3 + 3\mathbf{b}_3)/7 & \mathbf{a}_3 = (-8\mathbf{a}_1 - 3\mathbf{b}_1)/7 \\ \mathbf{b}_1 = (-3\mathbf{a}_3 - 8\mathbf{b}_3)/7 & \mathbf{b}_3 = (3\mathbf{a}_1 - 5\mathbf{b}_1)/7 \\ \mathbf{c}_1 = \mathbf{c}_3 & \mathbf{c}_3 = \mathbf{c}_1 \\ \mathrm{Det} = +1 & \mathrm{Det} = +1. \end{array}$$

Note again that the latter transformations are not binary, *i.e.* their second powers are not the identity. The transformations of the Miller indices hkl are the same as those of the basis vectors (*cf.* §§6.1 and 6.2).

The authors are grateful to J. Thar and A. von Berg of the Institut für Kristallographie for the preparation of the figures and to two unknown referees whose comments considerably helped to improve the paper.

References

Arnold, H. (2002). *Transformations in Crystallography*, Part 5, *International Tables for Crystallography*, Vol. A, *Space-Group Symmetry*, edited by Th. Hahn, 5th ed., pp. 81, 84. Dordrecht: Kluwer.

Azruni, A. (1887). *Proc. Russ. Mineral. Soc. St Petersburg*, **23**, 126–132.

Bindi, L., Rees, L. H. & Bonazzi, P. (2003). *Acta Cryst.* B**59**, 156–158.

Bögels, G., Buijnsters, J. G., Verhaegen, S. A. C., Meekes, H., Bennema, P. & Bollen, D. (1999). *J. Cryst. Growth*, **191**, 446–454.

Bruker (2005). *Bruker Suite.* Bruker AXS Inc., Madison, WI, USA.

Buck, P. & Nagel, M. (1981). *Z. Kristallogr.* **157**, 292–298.

Buerger, M. J. (1956). *Elementary Crystallography*, ch. 10, *Crystal Forms*, pp. 122, 128, 134–135, 143–146, 161–162. New York: Wiley.

Buerger, M. J. (1960). *Crystal-Structure Analysis*, ch. 5, *Twinning*, pp. 53–68. New York: Wiley.

Davies, M. J., Smith, M. D. & zur Loye, H.-C. (2003). *Inorg. Chem.* **42**, 6980–6982.

Fregola, A. R., Melone, N. & Scandale, E. (2005). *Eur. J. Mineral.* **17**, 761–768.

Fregola, A. R. & Scandale, E. (2007). *Phys. Chem. Mineral.* **34**, 529–541.

Friedel, G. (1926). *Leçons de Cristallographie*, ch. 15, *Macles.* Nancy, Paris, Strasbourg: Berger-Levrault. [Reprinted 1964; Paris: Blanchard.]

Fritsch, E., Moore, M., Rondeau, B. & Waggett, R. G. (2005). *J. Cryst. Growth*, **280**, 279–285.

Gemmi, M., Merlini, M., Cruciani, G. & Artioli, G. (2007). *Am. Mineral.* **92**, 1685–1694.

Götz, D., Herres, N., Diehl, R. & Klapper, H. (2012). In preparation.

Grimmer, H. (1989*a*). *Acta Cryst.* A**45**, 320–325.

Grimmer, H. (1989*b*). *Acta Cryst.* A**45**, 505–523.

Grimmer, H. (2003). *Acta Cryst.* A**59**, 287–296.

Hahn, F. & Massa, W. (1997). *TWINXLI*. University of Marburg, Germany.

Hahn, Th. & Klapper, H. (2002). *Point Groups and Crystal Classes*, Part 10, *International Tables for Crystallography*, Vol. A, *Space-Group Symmetry*, edited by Th. Hahn, 5th ed. Dordrecht: Kluwer.

Hahn, Th. & Klapper, H. (2003). *Twinning of Crystals*, ch. 3.3, *International Tables for Crystallography*, Vol. D, *Physical Properties of Crystals*, edited by A. Authier. Dordrecht: Kluwer.

Herbst-Irmer, R. (2006). *Twinning*, ch. 7, *Crystal Structure Refinement*, edited by P. Müller, pp. 106–149. Oxford University Press.

Herbst-Irmer, R. & Sheldrick, G. M. (1998). *Acta Cryst.* B**54**, 443–449.

Herbst-Irmer, R. & Sheldrick, G. M. (2002). *Acta Cryst.* B**58**, 477–481.

Hettiarachchi, S. R., Schaefer, B. K., Yson, R. L., Staples, R. J., Herbst-Irmer, R. & Patterson, H. H. (2007). *Inorg. Chem.* **46**, 6997–7004.

Hu, X. B., Wang, J. Y., Tian, L. L., Guan, Q. C., Liu, Y. G., Wei, J. Q., Jiang, M. H., Liu, W. J., Jiang, S. S. & Jiang, J. H. (1998). *Phys. Status Solidi A*, **170**, 29–35.

Klapper, H. (1987). *Progress in Crystal Growth and Characterization*, Vol. 14, edited by P. Krishna, pp. 367–401. Oxford: Pergamon.

Klapper, H. & Hahn, Th. (2010). *Acta Cryst.* A**66**, 327–346.

Kotrbova, M., Kadeckova, S., Novak, J., Bradler, J., Smirnov, V. G. & Shvydko, Yu. V. (1985). *J. Cryst. Growth*, **71**, 607–614.

Lang, A. R. (1999). *International Tables for Crystallography*, Vol. C, *Mathematical, Physical and Chemical Tables*, edited by A. J. C. Wilson & E. Prince, 2nd ed., ch. 2.7, pp. 113–123. Dordrecht: Kluwer.

Machado, W. G., Moore, M. & Yacoot, A. (1998). *J. Appl. Cryst.* **31**, 777–782.

Moore, M. (2009). *J. Phys. Condens. Matter*, **21**, 364217.

Müller, U. (2004). *Relations Between the Wyckoff Positions*, Part 3, *International Tables for Crystallography*, Vol. A1, *Symmetry Relations between Space Groups*, edited by H. Wondratschek & U. Müller, p. 708. Heidelberg: Springer.

Nuss, J. & Jansen, M. (2007). *Acta Cryst.* B**63**, 843–849.

Oeckler, O., Bauer, J., Duppel, V., Mattausch, H. & Simon, A. (2002). *Acta Cryst.* B**58**, 161–167.

Panina, Z. V., Malinovskii, Yu. A., Kuz'micheva, G. M. & Zharikov, E. V. (1995). *Kristallografiya*, **40**, 645–649.

Rosenzweig, A. & Cromer, D. T. (1959). *Acta Cryst.* **12**, 709–712.

Sheldrick, G. M. (1997). *SHELXL97. Program for the Refinement of Crystal Structures from Diffraction Data.* University of Göttingen, Germany.

Sheldrick, G. M. (2008). *Acta Cryst.* A**64**, 112–122.

Shubnikov, A. V. & Koptsik, V. A. (1974). *Symmetry in Science and Art*, ch. 3, p. 73. New York: Plenum Press.

Tamazyan, R., Arnold, H., Molchanov, V. N., Kuzmicheva, G. M. & Vasileva, I. G. (2000). *Z. Kristallogr.* **215**, 346–351.

Tohno, S. & Katsui, A. (1986). *J. Cryst. Growth*, **74**, 362–374.

Tschermak, G. & Becke, F. (1921). *Lehrbuch der Mineralogie*, 8th ed., p. 603. Wien: Alfred Hölder.

Vainshtein, B. K. (1994). *Fundamentals of Crystals*, 2nd ed., ch. 3.2, pp. 184–188. Berlin: Springer.

Wallace, C. A. & White, E. A. D. (1967). *Crystal Growth*, edited by H. S. Peiser (Supplement to *Phys. Chem. Solids*), pp. 431–435. Oxford: Pergamon.

Wilkens, J. & Müller-Buschbaum, H. (1992). *J. Alloys Compd*, **184**, 195–201.

Yacoot, A., Moore, M. & Machado, W. G. (1998). *J. Appl. Cryst.* **31**, 767–776.

Yakubovich, O. V., Massa, W., Gavrilenko, P. G. & Pekov, I. V. (2005). *Crystallogr. Rep.* **50**, 544–553. [Translated from *Kristallografiya*, **50**, 595–604.]